

ข้อผิดพลาดด้วยแกรฟีน/พอลิแอนิซีนนาโนคอมพอสิตสำหรับใช้วินิจฉัยภาวะไตเสียหาย



บทคัดย่อและแฟ้มข้อมูลฉบับเต็มของวิทยานิพนธ์ตั้งแต่ปีการศึกษา 2554 ที่ให้บริการในคลังปัญญาจุฬาฯ (CUIR)  
เป็นแฟ้มข้อมูลของนิสิตเจ้าของวิทยานิพนธ์ ที่ส่งผ่านทางบัณฑิตวิทยาลัย

The abstract and full text of theses from the academic year 2011 in Chulalongkorn University Intellectual Repository (CUIR)  
are the thesis authors' files submitted through the University Graduate School.

วิทยานิพนธ์นี้เป็นส่วนหนึ่งของการศึกษาตามหลักสูตรปริญญาวิทยาศาสตรมหาบัณฑิต  
สาขาวิชาปิโตรเคมีและวิทยาศาสตร์พอลิเมอร์  
คณะวิทยาศาสตร์ จุฬาลงกรณ์มหาวิทยาลัย  
ปีการศึกษา 2557  
ลิขสิทธิ์ของจุฬาลงกรณ์มหาวิทยาลัย

GRAPHENE/POLYANILINE NANOCOMPOSITE MODIFIED ELECTRODE FOR ACUTE KIDNEY  
INJURY DIAGNOSIS



A Thesis Submitted in Partial Fulfillment of the Requirements  
for the Degree of Master of Science Program in Petrochemistry and Polymer Science  
Faculty of Science  
Chulalongkorn University  
Academic Year 2014  
Copyright of Chulalongkorn University

Thesis Title	GRAPHENE/POLYANILINE NANOCOMPOSITE MODIFIED ELECTRODE FOR ACUTE KIDNEY INJURY DIAGNOSIS
By	Miss Jutiporn Yukird
Field of Study	Petrochemistry and Polymer Science
Thesis Advisor	Professor Orawon Chailapakul, Ph.D.
Thesis Co-Advisor	Nadnudda Rodthongkum, Ph.D. Ratthapol Rangkupan, Ph.D.

---

Accepted by the Faculty of Science, Chulalongkorn University in Partial  
Fulfillment of the Requirements for the Master's Degree

.....Dean of the Faculty of Science  
(Professor Supot Hannongbua, Dr.rer.nat.)

THESIS COMMITTEE

.....Chairman  
(Associate Professor Vudhichai Parasuk, Ph.D.)

.....Thesis Advisor  
(Professor Orawon Chailapakul, Ph.D.)

.....Thesis Co-Advisor  
(Nadnudda Rodthongkum, Ph.D.)

.....Thesis Co-Advisor  
(Ratthapol Rangkupan, Ph.D.)

.....Examiner  
(Assistant Professor Duanghathai Pentrakoon, Ph.D.)

.....External Examiner  
(Associate Professor Weena Siangproh, Ph.D.)

จตุพร อยู่เกิด : ขั้วไฟฟ้าดัดแปรด้วยแกรฟีน/พอลิแอนิไลนนาโนคอมพอสิตสำหรับใช้วินิจฉัยภาวะไตเสียหาย (GRAPHENE/POLYANILINE NANOCOMPOSITE MODIFIED ELECTRODE FOR ACUTE KIDNEY INJURY DIAGNOSIS) อ.ที่ปรึกษาวิทยานิพนธ์หลัก: ศ. ดร.อรุวรรณ ชัยลภากุล, อ.ที่ปรึกษาวิทยานิพนธ์ร่วม: ดร.นาฏนัตดา รอดทองคำ, ดร.รัฐพล รังกุพันธ์, 53 หน้า.

งานวิจัยนี้ได้พัฒนาขั้วไฟฟ้ารูปแบบใหม่ ซึ่งดัดแปรขั้วไฟฟ้าใช้งานด้วยวัสดุนาโนคอมพอสิตของแกรฟีนและพอลิแอนิไลน โดยใช้เทคนิคอิเล็กโทรสเปรย์ เพื่อเพิ่มพื้นที่ผิวให้กับขั้วไฟฟ้า จากนั้นจะเพิ่มหมู่อะมิโนด้วยการทำอิเล็กโทรพอลิเมอร์ไรเซชันของแอนิไลนมอนอเมอร์ในการยึดติดกับตัวรับรู้ทางชีวภาพ เพื่อใช้ในการตรวจวัดโปรตีนบ่งชี้ทางชีวภาพของโรคไต (Nuetrophil gelatinase-associated lipocalin; NGAL) การศึกษาปัจจัยที่ควบคุมลักษณะทางสัณฐานวิทยาของขั้วไฟฟ้าและคุณสมบัติทางเคมีไฟฟ้าของขั้วไฟฟ้าที่ดัดแปร เช่น ความเข้มข้นของแอนิไลนมอนอเมอร์ และจำนวนครั้งในการสแกน สำหรับการทำอิเล็กโทรพอลิเมอร์ไรเซชัน ลักษณะทางสัณฐานวิทยาของขั้วไฟฟ้าสามารถศึกษาด้วยกล้องจุลทรรศน์อิเล็กตรอนแบบส่องกราด กล้องจุลทรรศน์อิเล็กตรอนแบบส่องผ่าน และกล้องจุลทรรศน์แบบแรงอะตอม สำหรับการศึกษสมบัติทางเคมีไฟฟ้าของขั้วไฟฟ้าที่ดัดแปรด้วยเทคนิคไซคลิกโวลแทมเมตรีของสารละลายมาตรฐานเฟอริ/เฟอโรไซยาไนด์ พบว่าขั้วไฟฟ้าที่ดัดแปรมีการตอบสนองทางเคมีไฟฟ้าสูงกว่าขั้วไฟฟ้าที่ไม่ได้ดัดแปร การนำขั้วไฟฟ้าที่ดัดแปรมาประยุกต์ใช้ในการตรวจวัดโปรตีนบ่งชี้ทางชีวภาพของโรคไต พบว่าขั้วไฟฟ้าที่ดัดแปรมีการเพิ่มขึ้นของพีคออกซิเดชัน เนื่องจากการจับกันของแอนติบอดีและโปรตีน ในการตรวจวัดโปรตีนบ่งชี้ทางชีวภาพของโรคไตด้วยเทคนิคแอมเพโรเมตรี ภายใต้สภาวะที่เหมาะสมพบว่า ความสัมพันธ์เชิงเส้นระหว่างความเข้มข้นของโปรตีน NGAL กับสัญญาณอยู่ในช่วงความเข้มข้น 50-500 นาโนกรัมต่อมิลลิลิตร มีขีดจำกัดการตรวจวัดอยู่ที่ 21.13 นาโนกรัมต่อมิลลิลิตร นอกจากนี้ระบบของขั้วไฟฟ้าที่ดัดแปรยังสามารถนำมาประยุกต์ใช้ในการตรวจวัดโปรตีนบ่งชี้ทางชีวภาพโรคไตในตัวอย่างปัสสาวะได้

สาขาวิชา ปีโตรเคมีและวิทยาศาสตร์พอลิเมอร์ ลายมือชื่อนิสิต .....

ปีการศึกษา 2557

ลายมือชื่อ อ.ที่ปรึกษาหลัก .....

ลายมือชื่อ อ.ที่ปรึกษาร่วม .....

ลายมือชื่อ อ.ที่ปรึกษาร่วม .....

# # 5571943323 : MAJOR PETROCHEMISTRY AND POLYMER SCIENCE

KEYWORDS: GRAPHENE / POLYANILINE / NEUTROPHIL GELATINASE-ASSOCIATED LIPOCALIN / ACUTE KIDNEY INJURY

JUTIPORN YUKIRD: GRAPHENE/POLYANILINE NANOCOMPOSITE MODIFIED ELECTRODE FOR ACUTE KIDNEY INJURY DIAGNOSIS. ADVISOR: PROF. ORAWON CHAILAPAKUL, Ph.D., CO-ADVISOR: NADNUDDA RODTHONGKUM, Ph.D., RATTHAPOL RANGKUPAN, Ph.D., 53 pp.

A novel electrochemical immunosensor based on graphene/polyaniline nanocomposite modified electrode is successfully developed for the detection of neutrophil gelatinase-associated lipocalin (NGAL), a biomarker of acute kidney injury (AKI). The modified electrodes are fabricated by electro spraying of graphene/polyaniline (G/PANI) nanocomposite to increase electrode surface area and conductivity followed by electropolymerization of aniline to enhance the amino group (-NH<sub>2</sub>) on the electrode surface for antibody functionalization. Here, the factors affecting the electrode surface area and electrochemical sensitivity, such as aniline concentration, and scan number of electropolymerization are investigated and optimized. The morphologies of modified electrodes are characterized by scanning electron microscopy (SEM), transmission electron microscope (TEM), and atomic force microscopy (AFM). The electrochemical characteristics of modified electrode are investigated using cyclic voltammetry (CV). The CV results show the substantial increase of both anodic and cathodic peak currents of [Fe(CN)<sub>6</sub>]<sup>3-/4-</sup> on the modified electrode compared to an unmodified electrode indicating the improved electrochemical sensitivity of the system. For immunosensor application, the electrochemical detection of NGAL relies on the increase of oxidation current during the binding between antigen (NGAL) and antibody. In this study, NGAL binds to NGAL antibody attached on electropolymerized aniline on the modified electrode. Under optimum condition, a linear relationship between oxidation current and NGAL concentration is found in a range of 50-500 ng/mL and a limit of detection is found to be 21.13 ng/mL. Eventually, the proposed system is applied for the detection of NGAL in biological fluid (e.g. urine).

Field of Study: Petrochemistry and Polymer Student's Signature .....  
 Science Advisor's Signature .....

Academic Year: 2014 Co-Advisor's Signature .....  
 Co-Advisor's Signature .....

## ACKNOWLEDGEMENTS

I would like to thank to my thesis advisor and co-advisors, Professor Dr.Orawon Chailapakul, Dr. Nadnudda Rodthongkum and Dr. Ratthapol Rangkupan for their support and advice on this thesis.

I would like also thank Associate Professor Vudhichai Parasuk, thesis committee chairman, Assistant Professor Duanghathai Pentrakoon and Associate Professor Weena Siangproh, the thesis committee member for their advice and invaluable comments.

I am grateful to the financial supports from the Thailand Research Fund (TRF), through the New Researchers Grant (TRG5680012) and the National Research University Project, Office of Higher Education Commission (WCU-026-AM-57)

I am grateful to all members of my researcher group for their kindness and great friendship.

Finally, I would like to thank my family for their love and support throughout my life.

## CONTENTS

	Page
THAI ABSTRACT .....	iv
ENGLISH ABSTRACT .....	v
ACKNOWLEDGEMENTS .....	vi
CONTENTS .....	vii
LIST OF FIGURES .....	xi
LIST OF TABLE .....	xiv
CHAPTER I INTRODUCTION.....	1
1.1 Introduction .....	1
1.2 Research Objective.....	2
1.3 Scope of research.....	3
CHAPTER II THEORY AND LITERATURE REVIEW .....	4
2.1 Sensor.....	4
2.1.1 Principle.....	4
2.1.2 Immunosensor .....	5
2.2 Electrochemical detection.....	6
2.3.1 Cyclic voltammetry.....	7
2.3.2 Amperometry .....	8
2.4 Electrode modification .....	8
2.4.1 Nanomaterials .....	9
2.4.2 Conductive polymer .....	10
2.5 Electrospraying technique.....	12
2.6 Acute Kidney injury.....	15

	Page
2.7 Neutrophil gelatinase-associated lipocalin.....	15
2.8 Enzyme-linked immunosorbent assay.....	17
2.8.1 Direct ELISA.....	17
2.8.2 Sandwich ELISA.....	17
CHAPTER III EXPERIMENTAL.....	19
3.1 Chemicals and materials.....	19
3.2 Apparatus.....	20
3.3 Preparation of solution.....	20
3.3.1 0.5 M Potassium chloride solution.....	20
3.3.2 5 mM Ferri/ferro cyanide solution.....	20
3.3.3 0.1 M Phosphate buffer solution pH 7.0.....	20
3.3.4 G/PANI composite solution.....	21
3.3.5 Aniline solution.....	21
3.3.6 Urine sample.....	21
3.4 Electrode preparation.....	21
3.4.1 Electrode modification.....	22
3.5 Electrochemical detection.....	23
3.5.1 Cyclic voltammetry.....	23
3.5.2 Amperometry.....	24
3.6 Determination of NGAL.....	24
3.7 The performance of electropolymerized aniline on G/PANI nanocomposite modified electrode.....	24
3.7.1 Calibration curve.....	24



	Page
3.7.2 Limit of detection.....	25
3.7.3 Limit of quantitation.....	25
3.8.4 Interference study.....	25
3.8 Real sample study.....	25
CHAPTER IV RESULTS AND DISCUSSIONS.....	26
4.1 Optimization of electrode modification.....	26
4.1.1 Scan rate.....	27
4.1.2 The number of cycles.....	28
4.1.3 Aniline monomer concentration.....	30
4.2 Electrode characterization.....	33
4.2.1 Physical characterization.....	33
4.2.2 Electrochemical characterization.....	36
4.3 The performance of the electropolymerized aniline on G/PANI nanocomposite modified electrodes.....	37
4.4 NGAL Detection.....	38
4.4.1 Cyclic voltammetry.....	38
4.4.2 Amperometry.....	40
4.5 Calibration curve.....	42
4.6 Interference study.....	43
4.7 Real sample.....	43
4.8 Reproducibility and stability.....	44
CHAPTER V CONCLUSION.....	45
5.1 Conclusion.....	45

5.2 Suggestion for future work.....	45
REFERENCES .....	46
VITA.....	53



## LIST OF FIGURES

Figure	Page
2.1 A Schematic representation of biosensor.....	4
2.2 Schematic representation of the electrochemical detection of enzyme-linked immunoassay (ELISA) with antigens immobilized onto a gold electrode.....	6
2.3 Potential excitation waveforms and output electrochemical responses for cyclic voltammetry.....	7
2.4 Potential excitation waveforms and output electrochemical responses for amperometry.....	8
2.5 Carbon based nanomaterials. ....	9
2.6 Generalized oxidative and non-oxidative doping of polyaniline. There are three oxidation states leucoemeraldine, emeraldine and pernigraniline .....	11
2.7 Mechanisms of the direct electron transfer between GOD and SPCE through graphene in PEDOT:PSS and glucose detection in reduction regime .....	12
2.8 Equipment setup for electro spraying Process.....	13
2.9 Fabrication of G/PVP/PANI nanocomposite modified paper based for cholesterol detection.....	14
2.10 Electrospinning fabrication of G/PANI/PS nanofibers .....	14
2.11 Overview of ELISA procedures for ANCA detection .....	17
2.12 Schematic of the developed GNP-based sandwich immunoassay procedure for human lipocalin-2. ....	18
3.1 The schematic drawing of the preparation procedure for the G/PANI .....	22
3.2 Electro spraying of G/PANI nanocomposite solution on a screen printed carbon electrode.....	23

<b>4.1</b> Schematic diagram of electropolymerized PANI on G/PANI modified electrode for NGAL detection.....	27
<b>4.2</b> Cyclic voltammograms of 1.0 mM $[\text{Fe}(\text{CN})_6]^{3-/4-}$ at various scan rate for electropolymerization of 0.1 M aniline and of the anodic peak current ( $i_{pa}$ ) obtained from the cyclic voltammetry of 1.0 mM $[\text{Fe}(\text{CN})_6]^{3-/4-}$ in 5 mM KCl.....	28
<b>4.3</b> Cyclic voltammograms of 1.0 mM $[\text{Fe}(\text{CN})_6]^{3-/4-}$ at various scan number for electropolymerization of 0.1 M aniline at 100 mV/s and of the anodic peak current ( $i_{pa}$ ) obtained from the cyclic voltammetry of 1.0 mM $[\text{Fe}(\text{CN})_6]^{3-/4-}$ in 5 mM KCl.....	29
<b>4.4</b> The SEM images of electropolymerization of aniline on G/PANI nanocomposite modified electrode in difference scan number, 2 cycles (a), 4 cycles (b), 8 cycles (c), and 10 cycles (d) with 5000x magnification.....	30
<b>4.5</b> Cyclic voltammogram of 1.0 nM $[\text{Fe}(\text{CN})_6]^{3-/4-}$ at various concentration of aniline monomer for electropolymerization on G/PANI nanocomposite modified electrode and anodic peak current obtain from cyclic voltammogram of 1.0 mM $[\text{Fe}(\text{CN})_6]^{3-/4-}$ .....	31
<b>4.6</b> The SEM images of unmodified electrode (a) and electropolymerization of aniline on G/PANI nanocomposite modified electrode in difference concentration of aniline, 0.01 M (b), 0.05 M (c), 0.1 M (d), and 0.2 M (e) with 5000x magnification...	33
<b>4.7</b> TEM image of random G distribution within the G/PANI nanocomposite and electron diffraction pattern of graphene.....	34
<b>4.8</b> SEM images of unmodified electrode and the electropolymerized aniline on G/PANI nanocomposite modified electrode with 5000x magnification. ....	35
<b>4.9</b> AFM images of unmodified electrode (a), G/PANI nanocomposite modified electrode (b), and electropolymerized aniline on G/PANI nanocomposite modified electrode (c). ....	36
<b>4.10</b> Cyclic voltammograms of 1.0 mM $[\text{Fe}(\text{CN})_6]^{3-/4-}$ at 100 mV/s with the unmodified screen-printed carbon electrode (green line), G/PANI nanocomposite	

modified carbon electrode (blue line) and electropolymerized aniline on G/PANI nanocomposite modified electrode (red line).....	37
<b>4.11</b> The relationship between the square root of scan rate ( $\mathbf{V}^{1/2}$ ) and peak currents.....	38
<b>4.12</b> Cyclic voltammogram of electropolymerized aniline on G/PANI nanocomposite modified electrode in the absent (Blue) and present (Red) of 90 ng/mL of NGAL in phosphate buffer solution (pH 7.0) at scan rate 50 mV/s.....	39
<b>4.13</b> Cyclic voltammogram of 200 ng/mL NGAL with unmodified electrode (blue), G/PANI nanocomposite modified electrode (red), electropolymerized aniline on G/PANI nanocomposite modified electrode (green). ....	40
<b>4.14</b> A hydrodynamic voltammograms of 200 ng/mL of NGAL (red line) and background (blue line) in 0.1 M PBS pH 7.0 at a 75 s measured on electropolymerized aniline on G/PANI nanocomposite modified electrode.....	41
<b>4.15</b> Hydrodynamic voltammogram of the signal-to-background ratios (S/B) at different detection potential (0.1-0.6 V).....	41
<b>4.16</b> The calibration curve for detection of NGAL in the concentration range of 50 – 500 ng/mL in 0.1 M PBS (pH 7.0) .....	42
<b>4.17</b> The interference effect of BSA in PB solution and 100 ng/mL of NGAL.....	43

## LIST OF TABLE

Table	Page
4.1 Determination of NGAL in human urine sample.....	44
4.2 Determination of NGAL in patient urine sample.....	44



# CHAPTER I

## INTRODUCTION

### 1.1 Introduction

Acute kidney injury (AKI) or acute renal failure (ARF) is defined as an abrupt in kidney function. AKI is characterized by a rapid reduction in kidney function resulting in a failure to maintain fluid, electrolyte and acid-base homeostasis [1-5]. Therefore, AKI sensor has been developed to increase the accuracy and sensitivity for treatment of patients. A loss of kidney function is discovered by measuring of the urine output. Previously, AKI was diagnosed by the determination of serum creatinine (SCr) [6-9]. However, the concentration of SCr is not significantly change until loss of at least 50% of kidney function [10-12]. Thus, it is seriously to investigate a new biomarker for AKI diagnosis. The biomolecules used as the injury markers for AKI consist of urinary interleukin-18 (IL-18), neutrophil gelatinase-associated lipocalin (NGAL), kidney injury molecule-1 (KIM-1), and cystatin C [13-15].

Neutrophil gelatinase-associated lipocalin (NGAL) is a promising novel AKI biomarker [16-18] because NGAL is easily detected in both human urine and blood [19, 20] and it increases in urine and plasma of surgery patients within 2-6 h. Thus, NGAL is selected as a useful biomarker for AKI diagnosis. Various analytical techniques have been used for the quantitative determination of NGAL such as western blot [18, 21], immunoblotting [10], and enzyme-linked immunosorbent assay (ELISA) [22, 23]. However, those techniques still have some limitations, such as expensive instrument and time consuming. To solve these problems, electrochemical technique has been focused. Electrochemical detection has become a technique of interest due to its highly sensitivity, portable field- based size, ease of use, and low cost. Moreover, the electrochemical technique can be used simultaneously for quantitative and qualitative analyses [24-26]. For electrochemical analyses, modification of working electrode is required to improve the surface area and electrochemical sensitivity. Electrospraying technique is selected for electrode modification because the small size of droplet can be created on the electrode

surface [27, 28] leading to increased electrode surface area and electrochemical sensitivity. Various nanomaterials have been used for electrode modification such as carbon based nanomaterial (e.g. graphene, carbon nanotube) and metal based nanoparticles. Graphene (G) is one of carbon-based nanomaterial that attracts a great attention due to its remarkable properties, large specific surface area, high electrochemical conductivity, high stability, and low cost [29-31]. To prevent the agglomeration of G, conducting polymer has been chosen to combine with G and enhance the conductivity of electrode. In this work, polyaniline (PANI) is selected because of its low cost, ease of synthesis, good environmental stability, reversible redox reaction and biocompatibility [32, 33]. Moreover, it processes a large number of amino groups facilitating the immobilization of biomolecules. To increase amino groups of PANI on the electrode surface, electropolymerization of aniline is selected to create PANI on the electrode surface.

Herein, a novel AKI sensor is developed by electro spraying of G/PANI nanocomposites followed by electropolymerization of aniline monomer on working electrode. The electropolymerized aniline on G/PANI nanodroplet modified electrode is used to produce a large number of amino groups on electrode surface for functionalization of NGAL capture antibody using EDC/NHS covalent coupling. Then the modified electrode is used for the determination of NGAL. The performances of the developed sensor are optimized and applied for the determination of NGAL in complex biological fluid, such as human urine.

## 1.2 Research Objective

Two main goals of this dissertation are:

1. To develop high surface area and high conductivity of electrode for biosensor application.
2. To apply this proposed electrochemical sensor for the determination of NGAL in real biological fluid.



### 1.3 Scope of research

In this study, a novel electrode based on G/PANI is developed for NGAL determination. Graphene/polyaniline nanocomposite solution is electrospayed on an electrode followed by electropolymerization of aniline by cyclic voltammetry. Then, the modified electrode is functionalized by NGAL capture antibody using EDC/NSH coupling. The factors that affect to the electrochemical sensitivity of modified electrode, such as concentration of aniline monomer, number of scan for electropolymerization, and scan rate for electropolymerization are investigated and optimized. Eventually, the developed system is applied for the determination of NGAL in real biological fluid (e.g. human urine).



## CHAPTER II

### THEORY AND LITERATURE REVIEW

In this chapter, definitions and basic principles for understanding in sensor and electrochemical analysis are explained. The nanomaterials for electrode modification, such as graphene and polyaniline are discussed. Finally, NGAL-a biomarker for acute kidney injury diagnosis is introduced.

#### 2.1 Sensor

##### 2.1.1 Principle

Biosensor is an analytical device that specifically designed for the analyses of biomolecules. It converts the concentration of analytes into the measurable signal by recognizing a biological component and transferring it to the transducer. A schematic diagram of basic biosensor is showed in Figure 2.1.

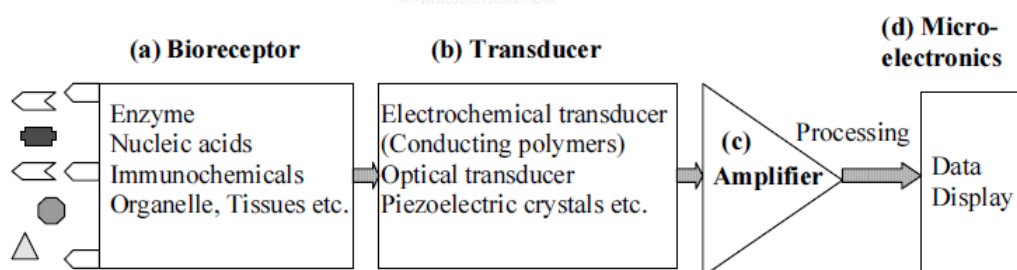


**Figure 2.1** A Schematic representation of biosensor [34].

The main components of biosensor consist of bioreceptor, transducer, amplifier, and microelectronics. For biosensor application, the bioreceptors such as enzyme, nucleic acid, immunochemical, organelle, and tissue recognize a specific analyte. Bioreceptors have been used as sensing probes in biosensor fabrications that connect with transducer. The transducer such as electrochemical transducer, optical transducer, and piezoelectric crystals

changed the signal resulting from the interaction of biological analyte and bioreceptor and biosensor reader device are amplify the signal respond.

Common types of sensors are resonant biosensor, optical-detection biosensor, thermal-detection biosensor, ion-sensitive FET biosensor and electrochemical biosensor. In this study, electrochemical sensor is selected due to its simplicity, sensitivity, portability, and high specificity.

### **2.1.2 Immunosensor**

The immunosensor is classified as optical, mass-sensitive or electrochemical according to the detection technique. The electrochemical immunosensor, according to the monitoring, is classified as amperometric, potentiometric, impedimetric and conductometric detection [35]. The specificity of the molecular recognition of antigen and antibody to form a stable complex is the basis. The concept of these analytical methods is based on the ligand-binding reaction between the target analyte. Antibodies are proteins generated by the immune system to identify bacteria, viruses, and parasites. The affinity between antibodies and antigens is very strong. Antibodies are immobilized in polymer matrix. The interaction of antibody and its target antigen changes in conductance, mass or optical properties, are detected directly with different transducers (Figure 2.2).

For electrochemical immunosensor, the interaction between antibody and antigen is converted to electrical signal, such as an electric current (amperometric immunosensor), a voltage difference (potentiometric immunosensor), or a resistivity change (conductimetric immunosensor) [36].

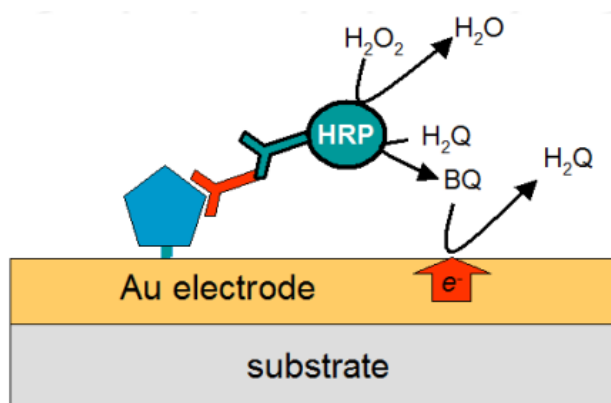


**Figure 2.2** Schematic representation of the electrochemical detection of enzyme-linked immunoassay (ELISA) with antigens immobilized onto a gold electrode [36].

## 2.2 Electrochemical detection

Electrochemical detection has become a technique of interest due to its highly sensitivity, portable field-based size, ease of use, and low cost. Moreover, the electrochemical technique can be used simultaneously for quantitative and qualitative analyses [24]. Electrochemistry is the study of the reduction and oxidation process of electroactive species. These reduction and oxidation reaction or redox reduction can provide about concentration, kinetic, reaction mechanism, and other department of species in solution. Electrochemical cells are differentiated into 2 types (potentiometry and potentiostatic). Potentiometry or galvanic cells are containing a spontaneous reaction, which based on electrodeposition of a charge potential in a zero current state. Potentiostatic technique is a dynamic (nonzero-current) process that stimulated an electrochemical cell with controlled potential and measured the current respond of electron-transfer reaction.

For sensor application, many methods based on potentiostatic techniques are used for electrochemical sensor such as cyclic voltammetry (CV), square-wave voltammetry (SWV), and amperometry. In this study, cyclic voltammetry and amperometry are used for electrochemical immunosensors.

### 2.3.1 Cyclic voltammetry

Cyclic voltammetry (CV) is widely used in electrochemical analysis and is a common electrochemical technique for initial study in electrochemical analysis. The electrochemical responses from CV show the redox properties of molecule in a solution [37]. For cyclic voltammetry (figure 2.3), the potential of working electrode is scanned from the initial potential ( $E^0$ ) to maximum potential ( $E^m$ ) at a fixed scan rate (V/s). Figure 2.3b shows cyclic voltammogram of a standard ferri/ferro cyanide ( $[\text{Fe}(\text{CN})_6]^{3-/4-}$ ), a reduction and oxidation of  $[\text{Fe}(\text{CN})_6]^{3-/4-}$  generate anodic and cathodic currents in and out of the working electrode [38, 39]. The anodic ( $i_{pa}$ ) and cathodic ( $i_{pc}$ ) current peaks can be used to predict electron transfer kinetic in the redox reaction. The peak current is directly proportional to the analyte concentration,  $C$ , and scan rate,  $v$ .

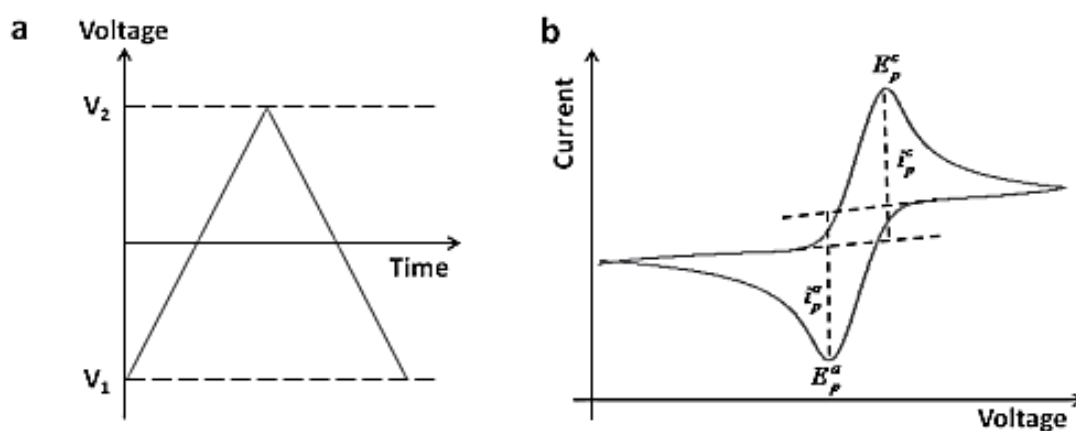


**Figure 2.3** Potential excitation waveforms and output electrochemical responses for cyclic voltammetry

The Randles–Sevcik equation predicts that the peak current should be proportional to the square root of the scan rate when voltammograms are taken at different scan rates.

$$i_p = (2.69 \times 10^5) n^{3/2} D^{1/2} \nu^{1/2} A C \quad (2.1)$$

Where	n:	the number of electrons appearing in half-reaction for the redox couple
	D:	The analyte's diffusion coefficient ( $\text{cm}^2/\text{s}$ )
	v:	Scan rate ( $\text{mV}/\text{s}$ )
	A:	The electrode area ( $\text{cm}^2$ )
	C:	concentration ( $\text{mol cm}^{-3}$ )

### 2.3.2 Amperometry

Amperometry is an electrochemical technique, which is very powerful for quantitative analysis. The current is recorded as a function of time, at a constant potential and the response signal is plotted between current and time. A diagram of waveform in a basic potential excitation step and chronoamperogram of the response from is showed in Figure 2.4.

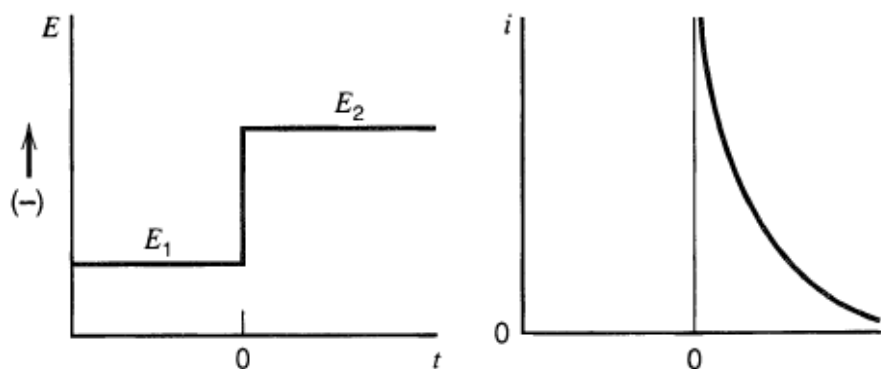


**Figure 2.4** Potential excitation waveforms and output electrochemical responses for amperometry [40].

## 2.4 Electrode modification

Electrochemical measurement is composed of three electrode system, reference electrode, counter electrode, and working electrode. The working electrode is the most important to enhance the electrochemical sensitivity and surface area. For electrochemical biosensor, working electrode is fabricated to small

size for make it portable. Nevertheless, the small size of working electrode limits the surface area and electrochemical sensitivity. Thus, modification of working electrode is required to improve the surface area and electrochemical sensitivity.

### 2.4.1 Nanomaterials

Various nanomaterials have been used for electrode modification such as carbon based nanostructures and metal based nanoparticles. In recent years, carbon nanomaterial has attracted a great attention due to its remarkable properties, i.e. large specific surface area, high electrochemical conductivity. Carbon nanomaterials such as carbon nanotube, carbon nanofiber, graphite, fullerene, and graphene have been used for electrode modification.

Graphene (G) is considered the basic building block of all graphitic forms including carbon nanotubes (CNTs), graphite and fullerene [30]. G is one of carbon-based nanomaterials that attracts a great attention due to its remarkable properties including large specific surface area, high electrochemical conductivity, high stability, and low cost. G possesses a single layer of carbon atom in a closely packed honey comb two dimensional lattice. G can be described as one-atom thick layers of graphite affect to lose of properties such as specific surface area and electrochemical conductivity [29].

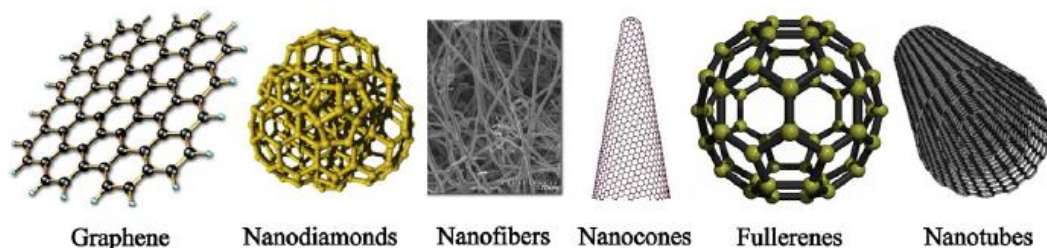


Figure 2.5 Carbon based nanomaterials [30].

## 2.4.2 Conductive polymer

In the recent studies, it has been reported that using conductive polymer for the dispersion of G can enhance the electrochemical sensitivity [26, 29]. Different conducting polymers have been used for electrode surface modification, such as polyaniline (PANI) [33, 41], polypyrrole (PPy) [42, 43], and poly(3,4- ethylenedioxythiophene) (PEDOT) [44, 45]. Among all, PANI is a promising material due to its low cost, ease of synthesis, good environmental stability, reversible redox reaction and biocompatibility.

The different structures of polyaniline are showed in Figure 2.6 including leucoemeraldine base (LEB), pernigraniline base (PNB), and emeraldine. The emeraldine form of polyaniline, is often referred to as emeraldine base (EB), with obtained in acidic condition and only conducting form due to the conjugate electron system and electron delocalization in ES to EB. EB is regarded as the most useful form of PANI due to its high stability at room temperature and moreover its doped form (emeraldine salt; ES) is electrically conducting [46].

PANI is an interesting material for biosensor interface because it can act as an effective mediator for electron transfer in redox or enzymatic reaction. Amino group of polyaniline are effective to binding and immobilization of biomolecules using covalent binding. The binding of amino group and analyte is detected the physical properties changes at the surface of electrode sensing.



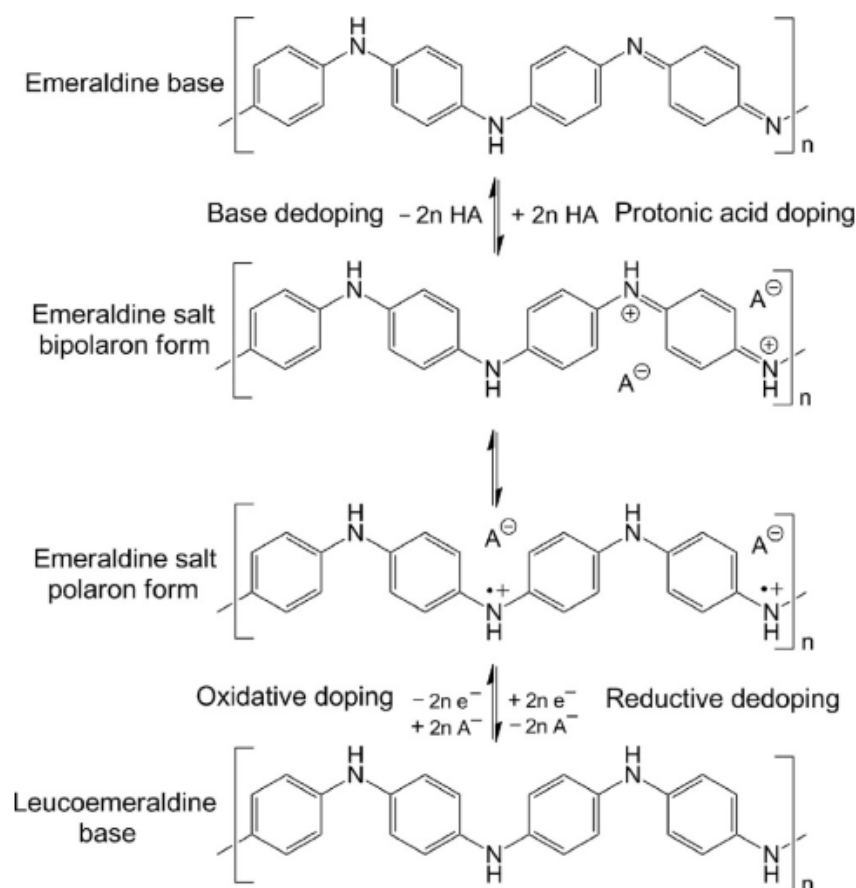


**Figure 2.6** Generalized oxidative and non-oxidative doping of polyaniline. There are three oxidation states leucoemeraldine, emeraldine and pernigraniline [47].

In the recent studies, the nanocomposites of G and conducting polymers are more compatible for electrode fabrication and biofunctionalization.

Wisitsoraat *et al.* [44] developed enzyme-based sensor using graphene-poly(3,4-ethylenedioxythiophene):polystyrene sulfonic acid (GP-PEDOT:PSS) modified screen printed carbon electrode (SPCE) for electrochemical detection of glucose. Glucose oxidase (GOD) enzyme is immobilized on GP-PEDOT:PSS by glutaraldehyde cross linking. The sensor shows good stability and sensitivity.

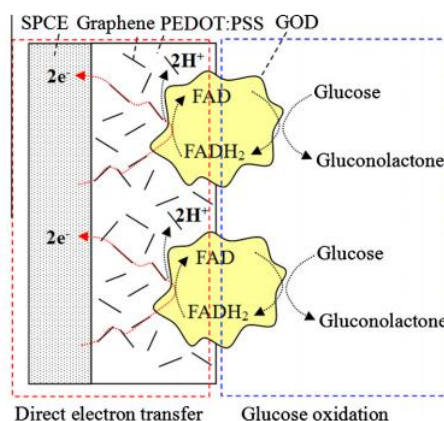


**Figure 2.7** Mechanisms of the direct electron transfer between GOD and SPCE through graphene in PEDOT:PSS and glucose detection in reduction regime [44].

Fan *et al.* [33] prepared an electrochemical sensor based on graphene-polyaniline (GR-PANI) nanocomposite for the determination of 4-aminophenol (4-AP). This sensor exhibits enhanced voltammetric response at GR-PANI modified GCE with high sensitivity.

Zhuang *et al.* [48] prepared overoxidized polypyrrole/graphene modified glassy carbon electrode (PPyox/graphene/GCE) for dopamine sensor. PPyox/graphene/GCE exhibits favorable electron transfer kinetics and electrocatalytic activity towards the oxidation of dopamine.

Xu *et al.* [49] developed a novel glucose biosensor using graphene/polyaniline/gold nanoparticles (AuNPs) nanocomposite modified glassy carbon electrode (GCE). The graphene/PANI/AuNPs nanocomposite is more biocompatible, high selective and sensitive determination of glucose with improved analytical capabilities.

## 2.5 Electro spraying technique

In this study, the electro spraying technique was employed to improve active surface area of the electrode.

The electrospaying process is a simple one-step technique that uses external electric field to induced charges, with similar polarity, on the surface of liquid droplet. For liquid with low molecular weight or a dilute polymer solution, the repulsive Coulombic force among these surface charges cause a large drop to break up into smaller droplets with size in the micro- to nanoscales [50]. The electrospaying process is conceptually simple; a polymer solution is loaded into syringe at a constant rate using syringe pump. Applying a high electrical force to polymer solution, the applied voltages used typically kilovolt up to 30 kV. The polymer solution is ejected from syringe needle to ground collector [51].

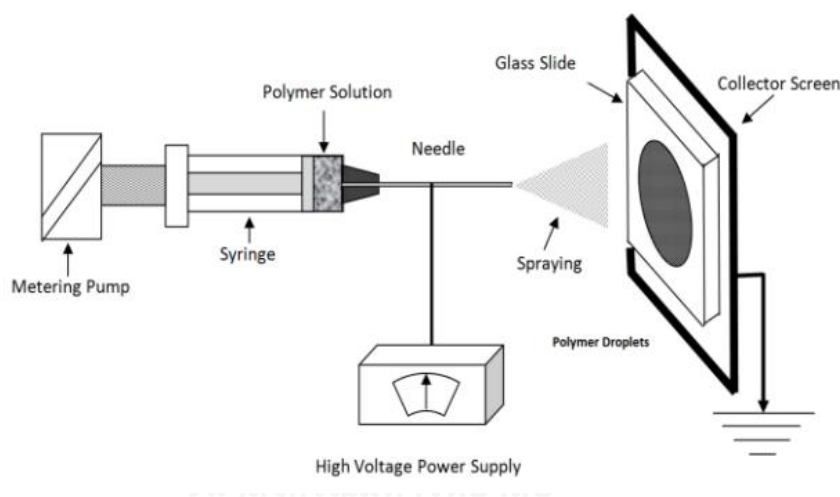


**Figure 2.8** Equipment setup for electrospaying Process

The electrospaying parameters are effect on droplet size and morphology such as viscosity, electrical conductivity, particle size, distribution, encapsulation efficiencies, loading capacities and in vitro release profiles [50]. Previous studies, electrospinning and electrospaying technique have been used for electrode modification.

Ruecha et al. [27] developed the electrochemical sensor using G/PVP/PANI nanocomposite modified paper based for cholesterol detection. The modified electrode also exhibits excellent electrocatalytic activity towards the oxidation of hydrogen peroxide ( $H_2O_2$ ).

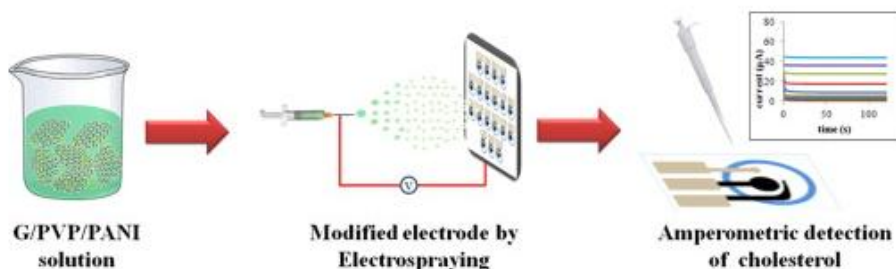


**Figure 2.9** Fabrication of G/PVP/PANI nanocomposite modified paper based for cholesterol detection [27].

Rodthongkum *et al.* [29] reported a highly sensitive electrochemical system based on electrospun graphene/polyaniline/polystyrene (G/PANI/PS) nanofiber-modified screen-printed carbon electrodes has been developed for dopamine (DA) determination. This G/PANI/PS modified electrode increased the surface areas and electrochemical sensitivity of system.

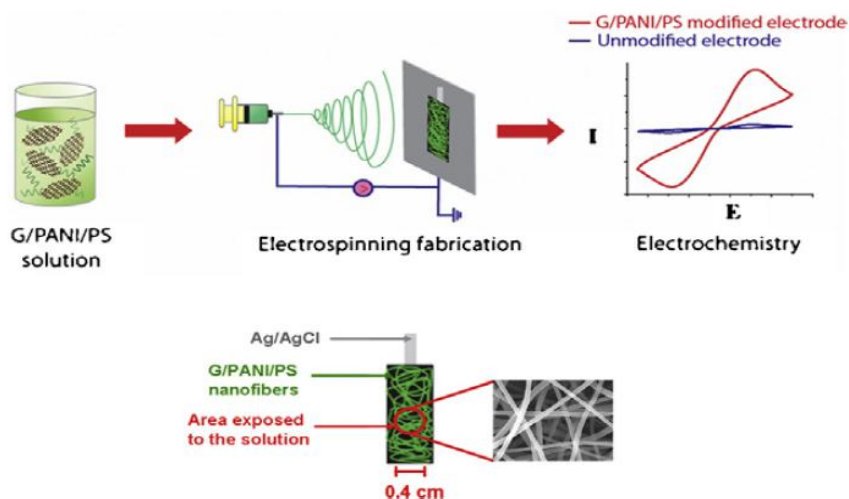


**Figure 2.10** Electrospinning fabrication of G/PANI/PS nanofibers [29].

Promphet *et al.* [26] fabricated G/PANI/PS porous nanofibers on the screen-printed carbon electrode for simultaneous lead and cadmium detection. The

electrospun G/PANI/PS nanoporous fiber showed the higher surface area than unmodified electrode and higher electrochemical sensitivity.

## 2.6 Acute Kidney injury

Acute kidney injury (AKI) or acute renal failure (ARF) has been reported in 5 to 7% of hospitalized patients [1-4], with a serious complication and an associated mortality rate in excess of 50% [22, 52, 53]. AKI is a loss of kidney function within over hours, days, and weeks. AKI is associated renal perfusion (42%), major surgery (18%), radiocontrast exposure (12%), and aminoglycoside administration (7%) [4, 54]. The factors are involved with kidney injury such as hemodynamic, inflammatory, and nephrotoxic. AKI increases the risk factor of death after cardiac surgery [55, 56]. Thus, AKI diagnosis has been developed to increase the accuracy and sensitivity for diagnosis and treatment of patients. A loss of kidney function is discovered by a measured in urine output.

Typically, AKI is diagnosed by the determination of serum creatinine (SCr) [6-9]. The minimal change of SCr increases the risk factor of death and decreases in survival. Unfortunately, the use of SCr to monitor kidney function has limitation for AKI diagnosis; the increase of SCr is insensitive, the concentration of SCr is not significantly change until loss of at least 50% of kidney function [10]. Thus, it is crucial to investigate a new biomarker for early AKI diagnosis. The biomolecules used as the injury markers for AKI are urinary interleukin-18 (IL-18), neutrophil gelatinase-associated lipocalin (NGAL), kidney injury molecule-1 (KIM-1), and cystatin C [13-15].

## 2.7 Neutrophil gelatinase-associated lipocalin

Neutrophil gelatinase-associated lipocalin (NGAL) is the most promising biomarker for diagnosis of AKI [16, 17]. NGAL is identified as a 25 kDa protein, covalently bound to gelatinase from human neutrophils. This protein is expressed at a very low concentration in human tissue, kidney, lung, stomach, and colon [18, 21, 22, 57]. NGAL is commonly found in both human urine and human blood. The extent

of NGAL increases in serum of patients with infection, asthma or pulmonary disease, and emphysematous lungs [13]. It is an important prognosis and diagnosis biomarker for several medical conditions [58]. The diagnosis using SCr expression usually takes 1 to 3 days after surgery but the increase of NGAL in both urine and plasma takes only 2-6 h. In general, NGAL concentration associates highly with SCr concentration [10] and NGAL concentration usually increases before SCr concentration [21]. In this study, NGAL is selected as a biomarker for early AKI diagnosis. Various analytical techniques have been reported for quantitative determination of NGAL, such as western blot [18, 21], immunoblotting [10], and enzyme-linked immunosorbent assay (ELISA) [22, 23].

Mishra *et al.* [18] studies children undergoing bypass, urine and blood samples were analysed by western blots and ELISA for NGAL expression. Concentrations in urine and serum of NGAL represent sensitive, specific, and highly predictive early biomarkers for acute renal injury after cardiac surgery.

Wagener *et al.* [10] studied cardiac surgical patients, NGAL analysis by quantitative immunoblotting. Urinary NGAL may therefore be a useful early biomarker of ARD after cardiac surgery.

However, these techniques require an expensive instrument and they are time consuming. To solve these problems, electrochemical technique is selected as an alternative tool for NGAL detection.

Electrochemical detection has become a technique of interest due to its high sensitivity, portable field- based size, ease of use, and low cost. Moreover, it can be used simultaneously for both quantitative and qualitative analyses. Nowadays, electrochemical sensor has been widely used in various application fields, such as food contaminant, environmental pollutant as well as clinical diagnosis [24, 25].

Kanan *et al.* [59] developed a label-free electrochemical immunosensor for the detection of neutrophil gelatinase-associated lipocalin (NGAL). The electrochemical immunosensor exhibited high sensitivity ( $1 \text{ ng mL}^{-1}$ ).

## 2.8 Enzyme-linked immunosorbent assay

Enzyme-linked immunosorbent assay (ELISA) is a conventional technique, used to measure the concentration of target analyte (e.g. protein) via antigen-antibody interaction. This technique has been commonly used for medical diagnosis.

### 2.8.1 Direct ELISA

Initially, antigen is adsorbed on the plate, then bovine serum albumin (BSA) is added to block other proteins. The enzyme-antibody complex is added to the plate and enzyme-antibody complex bind to antigen on the plate surface with antigen-antibody reaction. After, the excess enzyme-antibody complex is washed off using an appropriate buffer. The enzyme substrate is added and detected illustrating the signal of antigen.

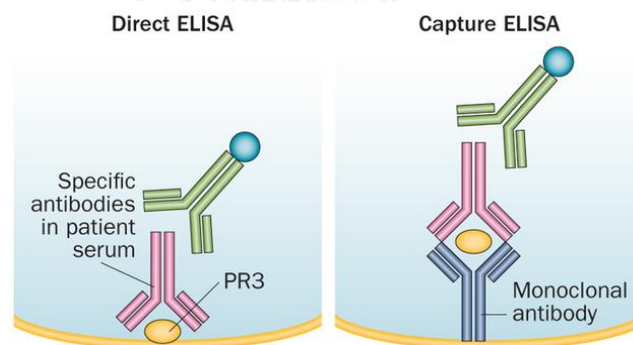
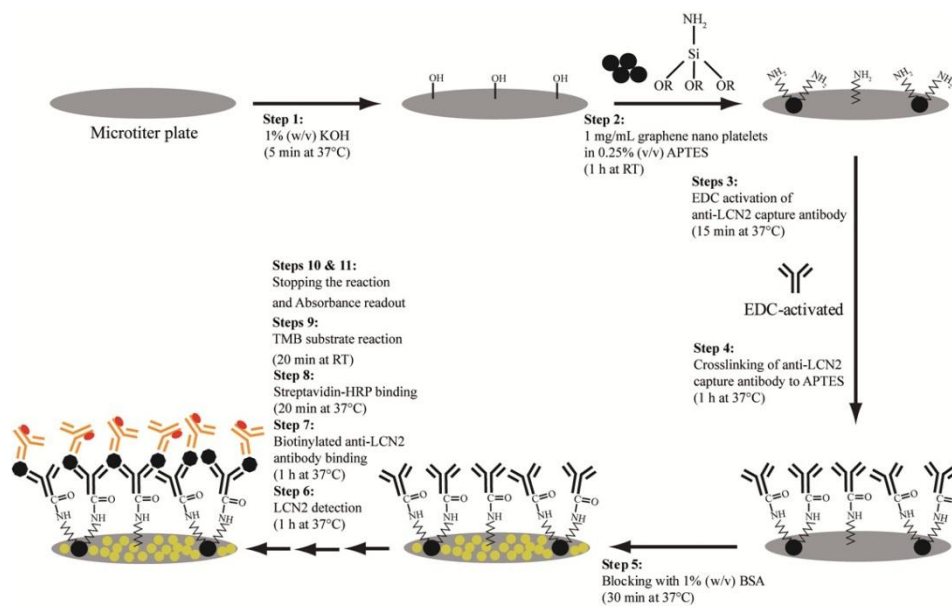


Figure 2.11 Overview of ELISA procedures for ANCA detection [60].

### 2.8.2 Sandwich ELISA

Antigen is immobilized on the plate. Then, sample is added to plate and binds to antigen with covalent bonding. Label detection antibody is added to the plate. The reaction of label detection antibody and substrate produces a detectable signal, most commonly a color change in the substrate.



**Figure 2.12** Schematic of the developed GNP-based sandwich immunoassay procedure for human lipocalin-2.

Vashist *et al.* [58] developed a highly sensitive immunoassay using graphene nano platelets (GNPs) on ELISA plate for the rapid detection of human lipocalin-2 (LCN2). The developed immunoassay correlated well with the conventional ELISA.



## CHAPTER III

### EXPERIMENTAL

#### 3.1 Chemicals and materials

3.1.1 Graphene nanopowders were purchased from SkySpringNanomaterials. Inc, (Houston, TX, USA).

3.1.2 The NGAL and capture NGAL antibody were purchased from R&D system and used as received.

3.1.3 Polyaniline emeraldine base ( $M_w = 65,000$ ), (+)-camphor-10-sulfonic acid (CSA), polystyrene ( $M_w = 180,000$ ), potassium ferricyanide ( $K_3[Fe(CN)_6]$ ), potassium ferrocyanide ( $K_2[Fe(CN)_6]$ ), 1-ethyl-3-(3-dimethylaminopropyl) carbodiimide (EDC), N-hydroxysuccinimide (NHS) were purchased from Sigma-Aldrich (St, Louis, MO, USA).

3.1.4 Potassium dihydrogen phosphate ( $KH_2PO_4$ ), chloroform, dichloromethane, N,N-dimethylformamide (DMF) were obtained from Carlo Erba Reagents (Milano, Italy).

3.1.5 Disodium hydrogen phosphates ( $Na_2HPO_4$ ), potassium chloride (KCl) were purchased from Merck (Darmstadt, Germany).

3.1.6 Carbon ink and silver/silver chloride ink were obtained from Gwent group (Torfaen, United Kingdom).

3.1.7 Filter paper (grade no.1, 46x57 cm) was purchased from Whatman.

3.1.8 Phosphate buffered solution (PBS) was prepared by dissolving 0.144% (w/v)  $Na_2HPO_3$ , 0.024% (w/v)  $KH_2PO_4$  in MilliQ water.

All solutions were prepared using DI water from MilliQ water system (Millipore, USA,  $R > 18.2 M\Omega cm^{-1}$ )

## 3.2 Apparatus

All electrochemical measurements including cyclic voltammetry and amperometry were performed on a  $\mu$ AUTOLAB type III potentiostat (Metrohm Siam Company Ltd., Switzerland) controlled by the General Purpose Electrochemical System (GPES) software. A three of electrode system was fabricated and used in this work. A screen-printed carbon electrode with 4 mm diameter was used as a working electrode (WE). For electrode modification, electrospraying and cyclic voltammetry were selected for modification of G/PANI nanocomposite, and electropolymerization of aniline, respectively. A JSM-6400 field emission scanning electron microscope (Japan Electron Optics Laboratory Co., Ltd, Japan) with an accelerating voltage of 15 kV and JEM-2100 transmission electron microscope (Japan Electron Optics Laboratory Co., Ltd, Japan) were used for the electrode characterization.

## 3.3 Preparation of solution

### 3.3.1 0.5 M Potassium chloride solution

Potassium chloride (KCl) solution was used as supporting electrolyte of a standard ferri/ferro cyanide  $[\text{Fe}(\text{CN})_6]^{3-/4-}$ , prepared by dissolving KCl (9.32 g) in 250 mL DI water

### 3.3.2 5 mM Ferri/ferro cyanide solution

0.1646 g potassium ferricyanide ( $\text{K}_3[\text{Fe}(\text{CN})_6]$ ) and 0.2112 g potassium ferrocyanide ( $\text{K}_4[\text{Fe}(\text{CN})_6]$ ) were mixed and dissolved in 100 mL of 0.5 M KCl.

### 3.3.3 0.1 M Phosphate buffer solution pH 7.0

1.4051 g potassium dihydrogen phosphate ( $\text{KH}_2\text{PO}_4$ ) and 2.0833 g disodium hydrogen phosphates ( $\text{Na}_2\text{HPO}_4$ ) were dissolved in 250 mL of DI water.

### 3.3.4 G/PANI composite solution

G/PANI nanocomposite solution was prepared by dispersing 2 mg/mL of G in DMF solution containing (2 mg/mL) of PVP, and then placing it in an ultrasonicator for 12 hr. For the preparation of PANI solution, 0.40 g of PANI emeraldine base was doped with 0.52 g camphorsulfonic acid and dissolved in chloroform. PANI solution was stirred at 1000 rpm for 6 h and filtered to obtain a clear PANI solution. Then, G and PANI solution were mixed together to provide G/PANI nanocomposite solution.

### 3.3.5 Aniline solution

Aniline monomer solution was used for electropolymerization. 0.1 M aniline solution was prepared by dilution of 0.229 mL 99.5% aniline in 25 mL of 0.5 M H<sub>2</sub>SO<sub>4</sub>.

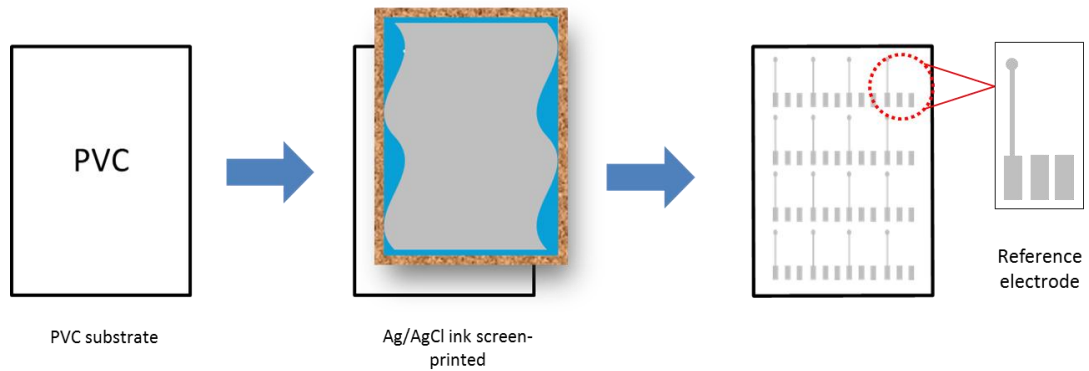
### 3.3.6 Urine sample

Urine sample was collected from the human. After collection, the human urine samples were centrifuge at 1600 rpm (Cole-Parmer, USA) for 20 min and then the supernatants were kept for further analyses.

## 3.4 Electrode preparation

A three-electrode system (working, counter, and reference) was fabricated on a polyvinyl chloride (PVC) substrate using a screen-printing technique. The patterned electrode was designed by Adobe Illustrator, and an ink-blocking stencil was fabricated by Chaiyaboon Co. (Bangkok, Thailand). Firstly, silver/silver chloride ink was screened on the PVC substrate as a reference electrode and conductive pad. Then, carbon ink was screened on the top of patterned silver/silver chloride layer as a working and counter electrode as showed in Figure 3.1. Finally, the screen-printed electrode was placed in the oven at 50 °C for 1 h to remove the remaining solvent.

### Step I. Ag/AgCl ink screen-printed



### Step II. Carbon ink screen-printed

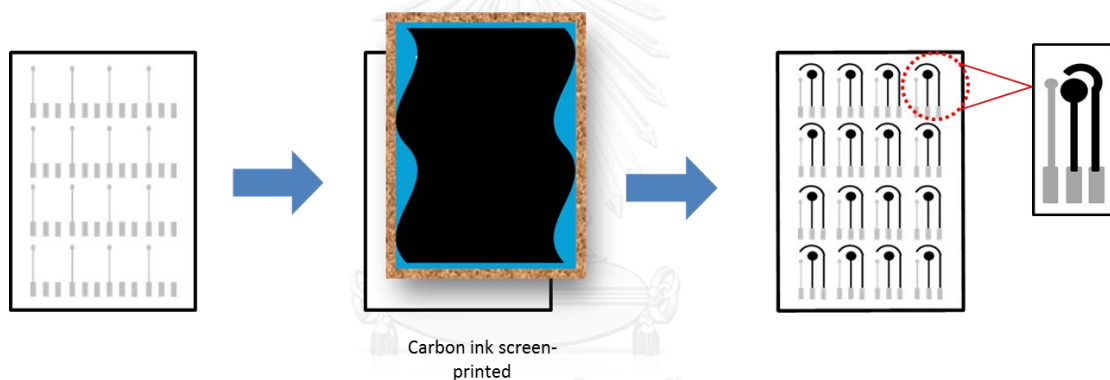


**Figure 3.1** The schematic drawing of the preparation procedure for the G/PANI

#### 3.4.1 Electrode modification

Electrospraying was selected for electrode modification by G/PANI nanocomposite solution. For electropolymerization of aniline on G/PANI modified electrode, cyclic voltammetry was employed.

##### 3.4.1.1 Electro spraying of G/PANI nanocomposite

G/PANI nanocomposite solution was prepared by mixing G and PANI solution, and it was used for electrode modification by electro spraying. The nanocomposite solution of G/PVP/PANI was added in a syringe and applied a high voltage at 7.5 kV to the

solution. The flow rate for electro spraying was controlled at 1.0 mL/h and a distance between needle and collector is fixed at 5 cm.

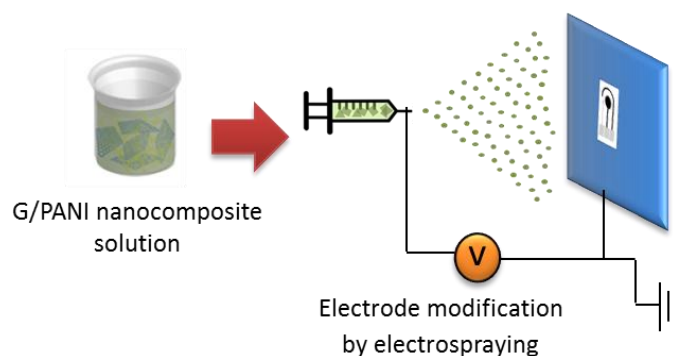


**Figure 3.2** Electro spraying of G/PANI nanocomposite solution on a screen printed carbon electrode.

#### 3.4.1.2 Electropolymerization of aniline

Electropolymerization of aniline on G/PANI modified electrode by CV was carried out. The factors affecting the modified electrode surface area and electrochemical sensitivity, such as aniline monomer concentration and scan number of electropolymerization were studied. The concentration of aniline was investigated in a range of 0.01 – 0.10 M. The number of scan was performed in a range of 2 to 10 cycles with 100 mV/s scan rate and a potential range of -0.5 to +1.0 V.

### 3.5 Electrochemical detection

All the electroanalytical measurements were performed on a  $\mu$ AUTOLAB type III potentiostat (Metrohm Siam Company Ltd.) with a three-electrode system.

#### 3.5.1 Cyclic voltammetry

For cyclic voltammetric measurement, the potential was scan from -0.5 V to +1.0 V for electropolymerization of aniline monomer, -0.5 V to +0.1 V for ferri/ferrocyanide detection and -0.2 V to +0.6 V for NGAL detection.

### 3.5.2 Amperometry

A hydrodynamic voltammetry was studied to optimize the detection potential of NGAL in a range of 0.1-0.6 V. The current are measured with different potentials and a suitable potential is selected. Then, the anodic current was recorded at a constant time of 75s.

### 3.6 Determination of NGAL

A modified electrode was developed for biological immobilization, amino group (-NH<sub>2</sub>) on the surface of the modified electrode was used for functionalization of NGAL antibody by covalent bonding using EDC/NHS coupling. To immobilize NGAL antibody on the modified electrode, EDC, NHS and NGAL antibody was mixed together in a ratio of 1:1:1, and dropped on the modified electrode surface. Then, it was incubated in a dark area for 3 h at a room temperature. After that, the excessed antibody was removed by using PBS and DI water, respectively. For NGAL detection, the solution of NGAL was dropped onto the electrode surface, and incubated for 30 min at room temperature; NGAL is detected due to the interaction between antibody and antigen. Before detection, the immobilized electrode was washed using PBS and DI water to remove the un-binding antigen-antibody. Finally, 0.1 M PBS (pH 7.0) was dropped on electrode for the determination of NGAL using electrochemistry.

### 3.7 The performance of electropolymerized aniline on G/PANI nanocomposite modified electrode

#### 3.7.1 Calibration curve

The electrochemical responses of electropolymerized aniline on G/PANI nanodroplet modified electrode were measured at different concentration of NGAL in a range of 50-500 ng/mL. For amperometric detection, the amperometric responses were record at 75 s as a steady

state. The calibration curve of NGAL was created by plotting between the amperometric responses at different concentration of NGAL.

### 3.7.2 Limit of detection

Limit of detection (LOD) was calculated by using  $LOD=3S_b/m$  equation, when  $S_b$  is a standard deviation of the blank (estimated by five replicates determination of the blank signals) and  $m$  is a slope of calibration curve.

### 3.7.3 Limit of quantitation

Limit of detection (LOD) was calculated using the equation of  $LOD=10S_b/m$ , when  $S_b$  is a standard deviation of the blank (estimated by five replicates determination of the blank signals) and  $m$  is a slope of calibration curve.

### 3.8.4 Interference study

Many substances such as bovine serum albumin (BSA) interfere the detection of NGAL in human urine sample. Therefore, the selectivity of the modified electrode was studied. For the assessment of BSA interference, the amperometric response of NGAL in the presence of BSA was measured and compared with background and NGAL signal.

## 3.8 Real sample study

Standard addition method was selected for the detection of NGAL in urine sample. The standard solutions of the NGAL were added into undiluted human urine samples in a ratio of 1:1. All samples were analyzed on electropolymerized aniline on G/PANI nanocomposite modified electrode using amperometric detection.

## CHAPTER IV

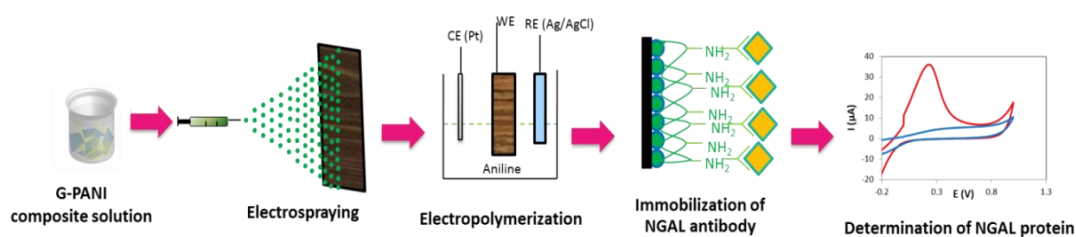
### RESULTS AND DISCUSSIONS

In this chapter, the results of preparation of electropolymerized aniline on G/PANI nanocomposite modified electrode and NGAL determination are discussed. These results including factors affecting for electropolymerization and electrochemical sensitivity of modified electrode, electrode surface morphology, analytical performance of modified electrode, interference study, and real sample analysis are studied and discussed

#### 4.1 Optimization of electrode modification

A novel electrochemical immunosensor based on G/PANI nanocomposites has been developed for the sensitive determination of NGAL as a biomarker for AKI diagnosis. The modified electrodes were prepared by electrospraying of G/PANI nanocomposites to increase the surface area and electrochemical sensitivity of working electrode. Then, electropolymerization of aniline monomer was used to generate PANI film on G/PANI nanocomposite modified electrode for increasing the electrochemical conductivity and creating the amino groups on the modified electrode for capture antibody functionalization. The schematic diagram of electropolymerized PANI on G/PANI nanocomposite modified electrode for NGAL detection was shown in Figure 4.1. The electrospraying parameters were optimized as shown in the previous report [27]. In this work, the parameters of electropolymerization of aniline by CV including number of cycle (scan number) and aniline monomer concentration were studied and optimized.

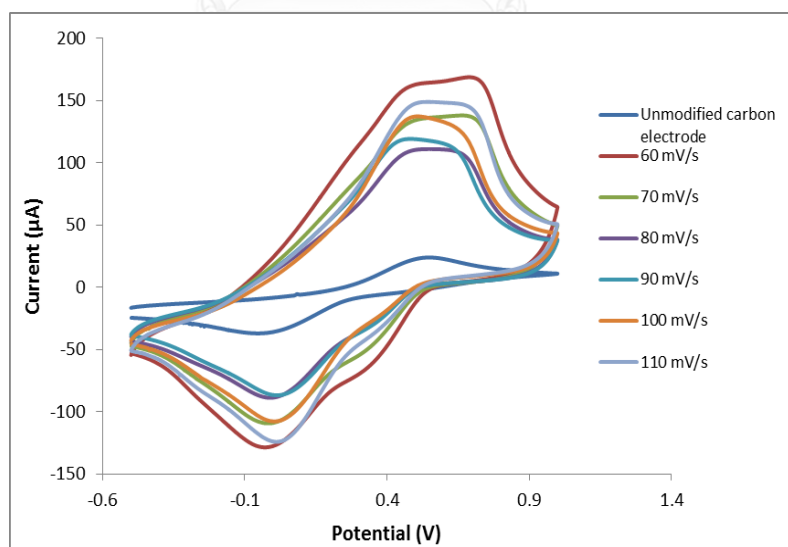




**Figure 4.1** Schematic diagram of electropolymerized PANI on G/PANI modified electrode for NGAL detection.

#### 4.1.1 Scan rate

To study the effect of scan rate for electropolymerization, potential cycling was applied between  $-0.5$  to  $1.0$  V at various scan rates for electropolymerization ( $60 - 110$  mV/s) in  $0.1$  M aniline for 4 cycles. The scan rate is related to the formation and growth of polyaniline on the electrode surface. Scan rate controls the polymerization of aniline monomer and the amount of amino groups on the electrode surface. In this study, scan rate plays a less important role on the sensor performance (Figure 4.2). A constant scan rate of  $100$  mV/s is selected for further experiments.



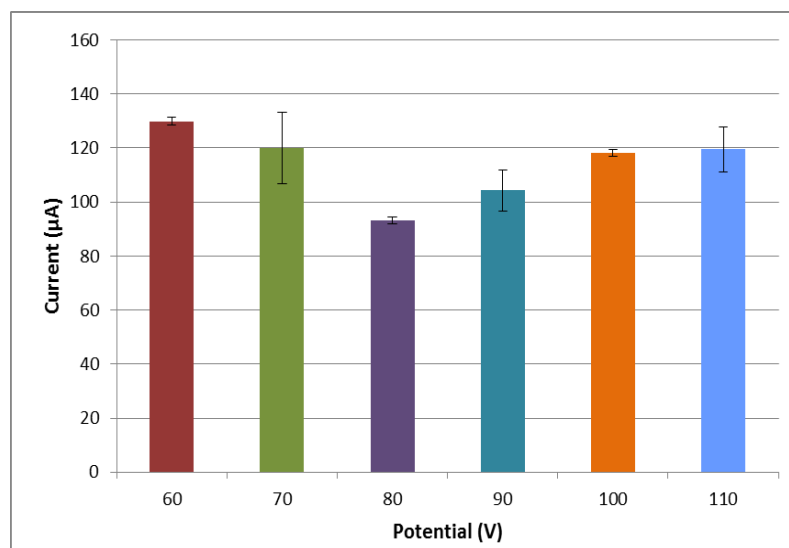


**Figure 4.2** Cyclic voltammograms of 1.0 mM  $[\text{Fe}(\text{CN})_6]^{3-/4-}$  at various scan rate for electropolymerization of 0.1 M aniline and of the anodic peak current ( $i_{pa}$ ) obtained from the cyclic voltammometry of 1.0 mM  $[\text{Fe}(\text{CN})_6]^{3-/4-}$  in 5 mM KCl.

#### 4.1.2 The number of cycles

One of the most important parameters for enhancing the surface area and electrochemical conductivity of electropolymerized PANI on G/PANI nanocomposite modified electrode is the number of cycle.

The number of cycle for electropolymerization of aniline controls the thickness of PANI on the modified electrode surface. The number of cycle was studied in a range of 2 to 10 cycles in 0.1 M aniline at 100 mV/s as shown in Figure 4.3. The anodic peak currents of standard ferri/ferrocyanide ( $[\text{Fe}(\text{CN})_6]^{3-/4-}$ ) increase when the number of cycle increase with 4 cycles of scan having the highest anodic peak current. When the number of cycle increases more than 4 cycles, the oxidation peak of polyaniline, at 0.8-0.9 V observed on the modified electrode surface. However, the peak potential difference values ( $\Delta E_p$ ) of the modified electrode also increases indicating longer rate of electron transfer kinetic, which lead to undesirable peak broaden. The  $\Delta E_p$  could be attributed to an increase of PANI layer thickness on electrode surface at higher scan cycles (Figure 4.4). Therefore, four cycles was chosen for electropolymerization of aniline in this study.

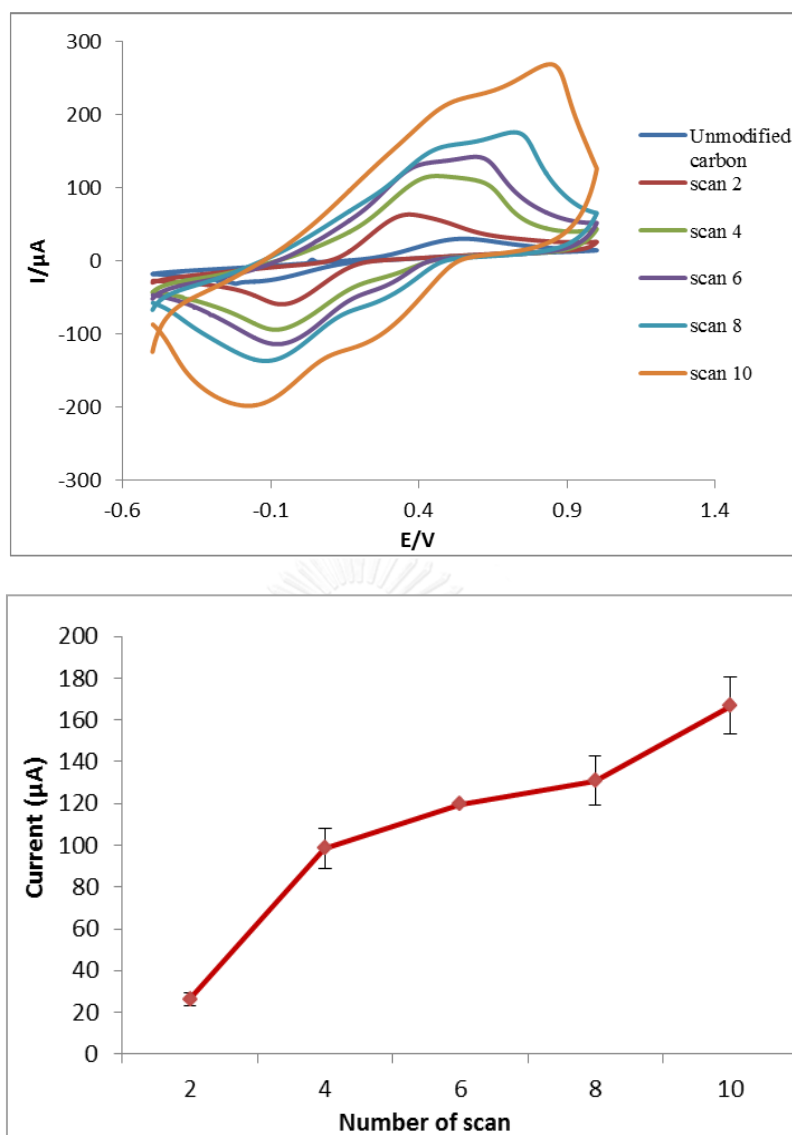


**Figure 4.3** Cyclic voltammograms of 1.0 mM  $[\text{Fe}(\text{CN})_6]^{3-/4-}$  at various scan number for electropolymerization of 0.1 M aniline at 100 mV/s and of the anodic peak current ( $i_{pa}$ ) obtained from the cyclic voltammometry of 1.0 mM  $[\text{Fe}(\text{CN})_6]^{3-/4-}$  in 5 mM KCl.

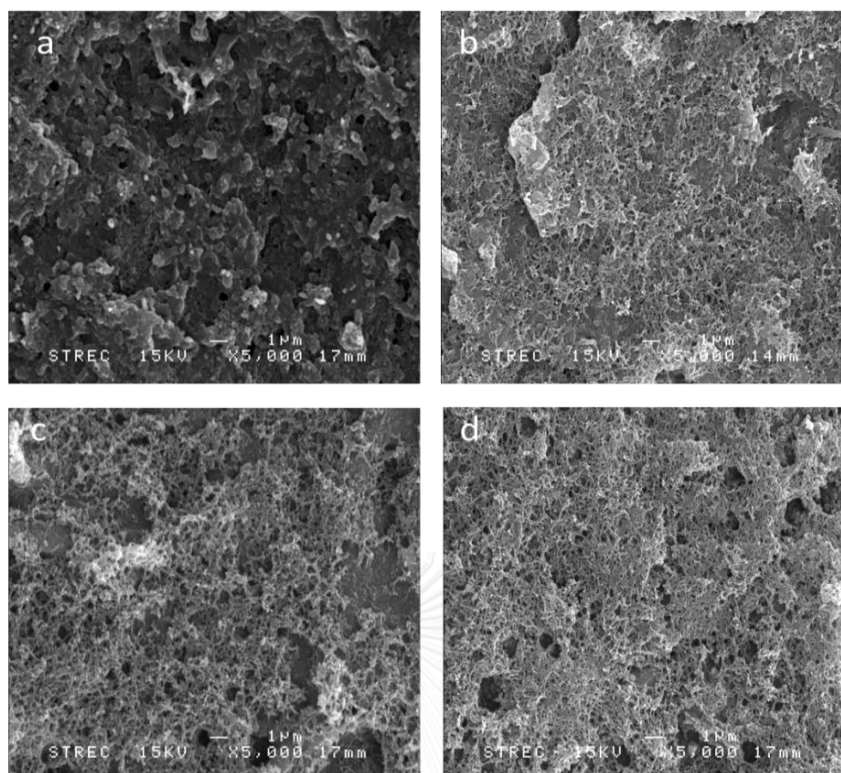
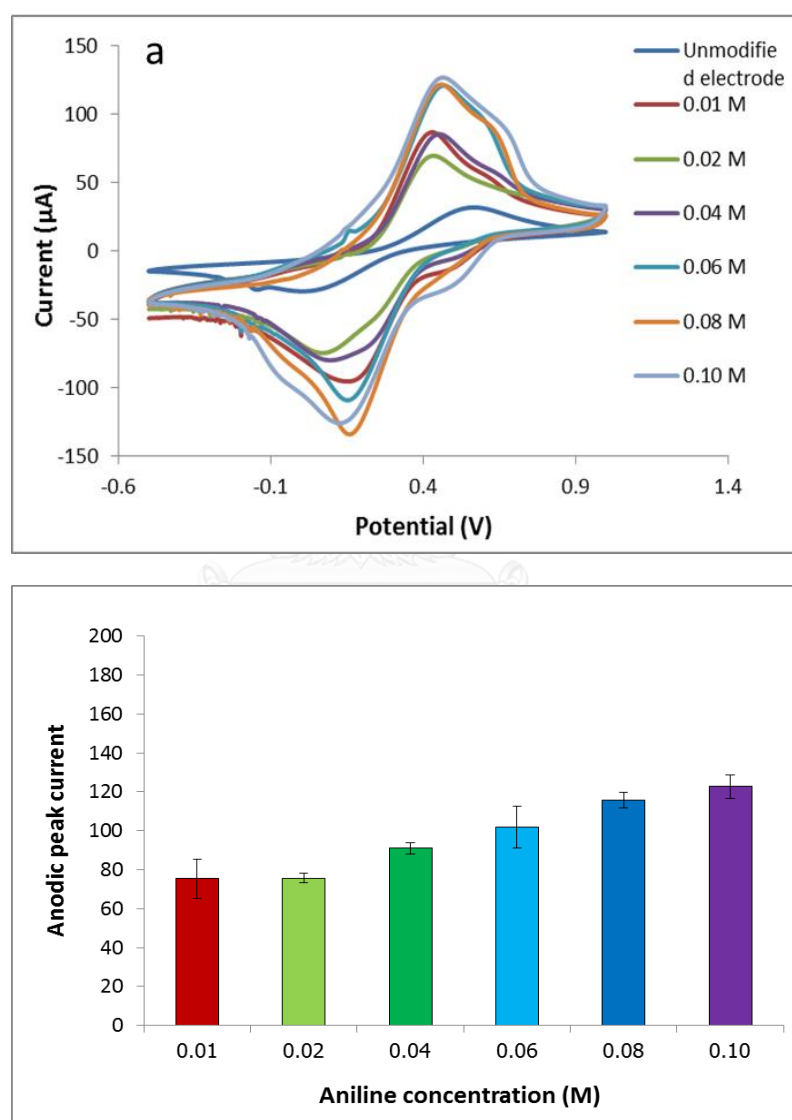


**Figure 4.4** The SEM images of electropolymerization of aniline on G/PANI nanocomposite modified electrode in difference scan number, 2 cycles (a), 4 cycles (b), 8 cycles (c), and 10 cycles (d) with 5000x magnification.

#### 4.1.3 Aniline monomer concentration

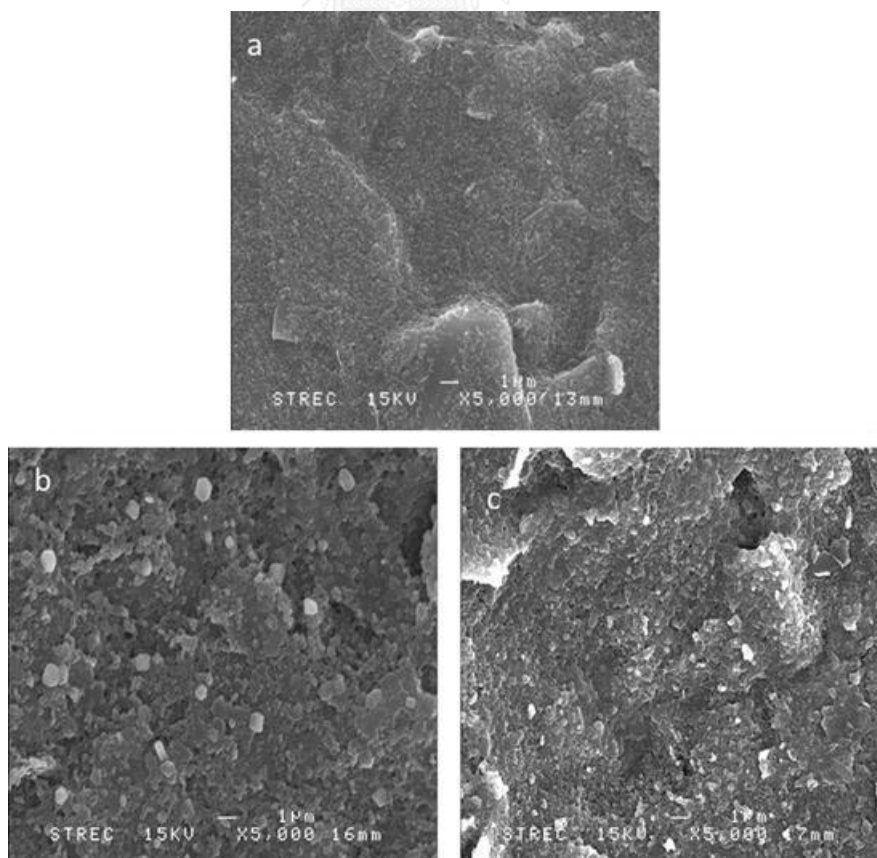
To study the effect of aniline concentration on the electrochemical sensitivity of electropolymerized aniline on G/PANI nanocomposite modified electrode, different concentrations of aniline monomer were investigated in a range of 0.01 – 0.10 M at scan rate 100 mV/s, 4 cycles. The cyclic voltammograms of 1.0 mM  $[\text{Fe}(\text{CN})_6]^{3-/4-}$  at different concentrations of aniline were shown in Figure 4.5. The increase of aniline concentration significantly increases the anodic peak current of 1.0 mM  $[\text{Fe}(\text{CN})_6]^{3-/4-}$  and electrochemical sensitivity of modified electrode due to when increased the concentration of aniline leading to polymerization of aniline monomer on the electrode surface. In this study, 0.10 M of aniline provided the highest anodic peak current, so, it was selected for the electropolymerization of aniline. Moreover, increasing the aniline concentration enhances the polyaniline on the

electrode surface and increased the electrochemical response. Unfortunately, the amount of polyaniline on the electrode surface risk of dislodged. Therefore, the concentration of aniline 0.10 M was chosen for electropolymerization in further experiments. The optimized parameters that were used for electropolymerization of aniline are 4 cycles of scan number and 0.10 M of aniline concentration at scan rate 100 mV/s.



**Figure 4.5** Cyclic voltammogram of 1.0 mM  $[\text{Fe}(\text{CN})_6]^{3-/4-}$  at various concentration of aniline monomer for electropolymerization on G/PANI nanocomposite modified electrode and anodic peak current obtain from cyclic voltammogram of 1.0 mM  $[\text{Fe}(\text{CN})_6]^{3-/4-}$ .

The morphology of modified electrode was characterized by SEM as shown in Figure 4.6. The unmodified carbon electrode surface appeared to be relatively smooth with nanoscopic droplets covered uniformly on it (Figure 4.6a). With 0.01 M aniline electropolymerization, numerous micro-particle structures, presumed to be polyaniline, of various shapes formed and distributed on the entire electrode surface, as shown in Figure 4.6b. The increase of aniline concentration from 0.01 M to 0.05 M led to a size reduction and apparent denser packing of these new surface structures, as shown in Figure 4.6c. Morphology of the surface changed significantly at 0.1 M aniline concentration where a fairly uniform of the polyaniline fibrous network, with numerous nanopores distributed homogenously on the film, appeared to cover the entire surface of the electrode. At higher concentration of aniline, the SEM image in Figure 4.6e showed thicker buildup of polyaniline fibrous layer on the electrode surface which can lead to decreased surface area of electrode and risk of dislodged.



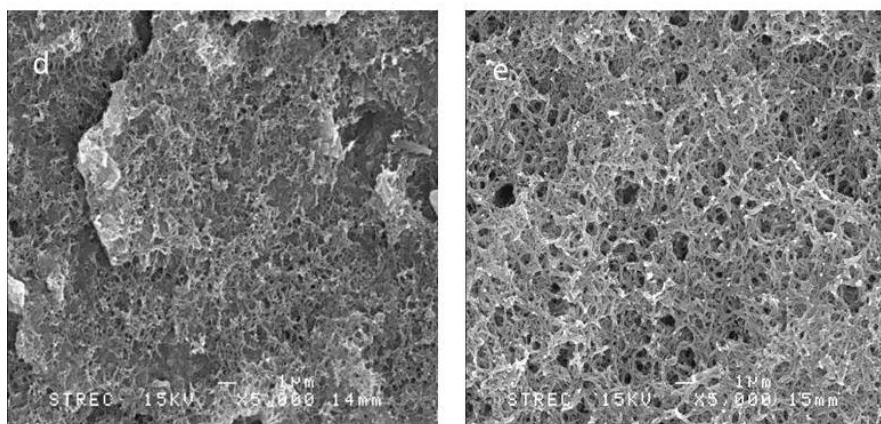
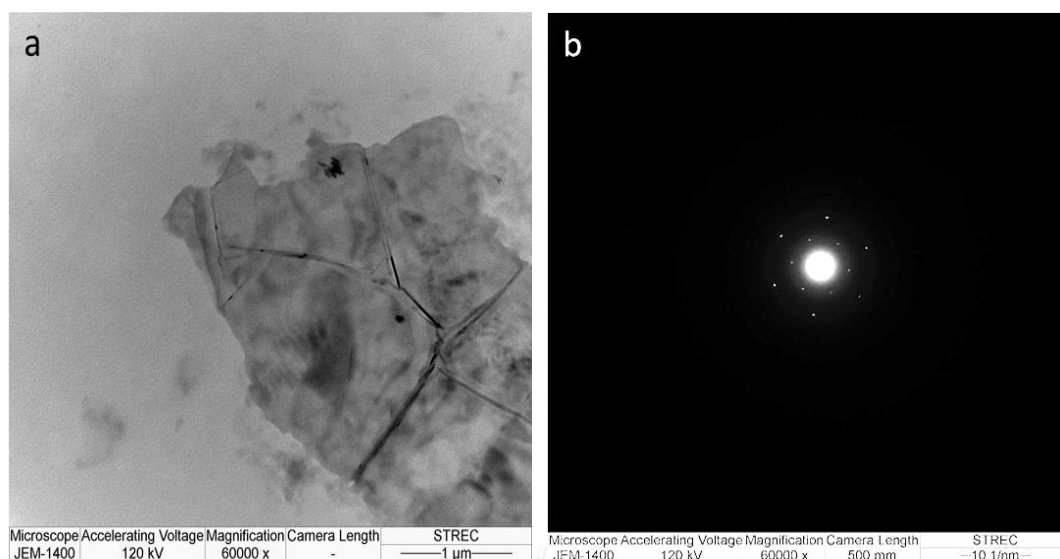


**Figure 4.6** The SEM images of unmodified electrode (a) and electropolymerization of aniline on G/PANI nanocomposite modified electrode in difference concentration of aniline, 0.01 M (b), 0.05 M (c), 0.1 M (d), and 0.2 M (e) with 5000x magnification.

## 4.2 Electrode characterization

### 4.2.1 Physical characterization

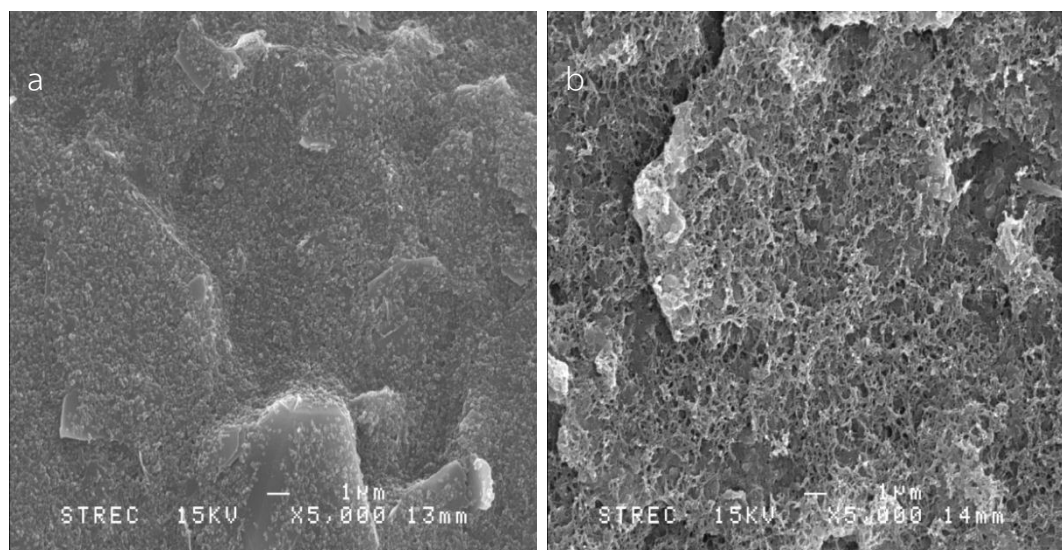
The dispersion of G on electrospayed G/PANI nanocomposite modified electrode was characterized by transmission electron microscopy (TEM). A TEM image (Figure 4.7a) confirms that G is randomly distributed and dispersed inside of nanocomposites without severe agglomeration, and the electron diffraction pattern of G (Figure 4.7b) is corresponded well with the previous report [31].



**Figure 4.7** TEM image of random G distribution within the G/PANI nanocomposite and electron diffraction pattern of graphene.

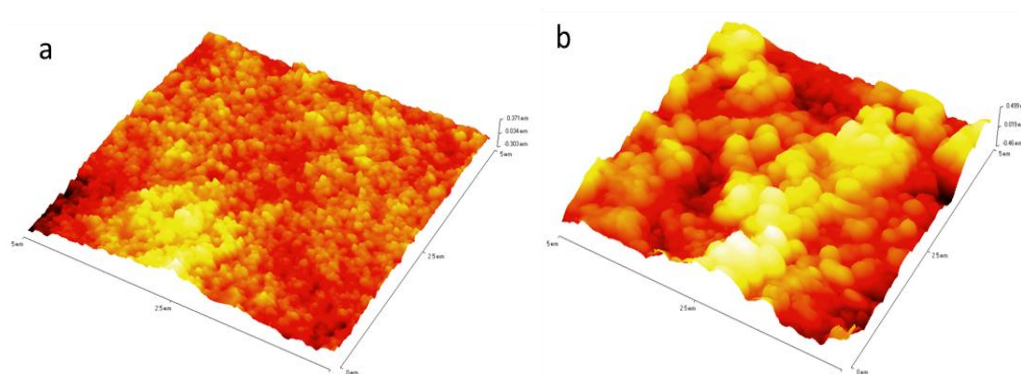
Moreover, the morphology of electropolymerized aniline on G/PANI nanocomposite modified electrode and unmodified electrode were characterized by scanning electron microscopy (SEM) as shown in Figure 4.8. The SEM images of electropolymerized aniline on G/PANI nanocomposite modified electrode showed a homogenous thickness and porous network when compared with unmodified electrode. The electropolymerized aniline on the G/PANI nanocomposite modified electrode was green color and strongly attached to the modified electrode surface. The 3D polymer growth and roughness morphology of polyaniline on the electrode surface can be uniformly generated on the modified electrode surface that was confirmed by SEM image (Figure 4.8b). PANI layer increases the amount of amino groups on the electrode surface, facilitating the biofunctionalization on the modified electrode surface in the next step of experiment.





**Figure 4.8** SEM images of unmodified electrode and the electropolymerized aniline on G/PANI nanocomposite modified electrode with 5000x magnification.

To characterize the surface of electropolymerized aniline on G/PANI nanocomposite modified electrode, atomic force microscopy (AFM) was selected. The AFM images of modified electrode showed higher surface area and higher roughness than unmodified and G/PANI nanocomposite modified electrode. The surface roughness of electropolymerized aniline on G/PANI nanocomposite modified electrode was found to be  $0.1566 \mu\text{m}$  (Figure 4.9c). For unmodified electrode and G/PANI nanocomposite modified electrode, the surface roughness was found to be  $0.0687 \mu\text{m}$  and  $0.1503 \mu\text{m}$ , respectively (Figure 4.9a and b).



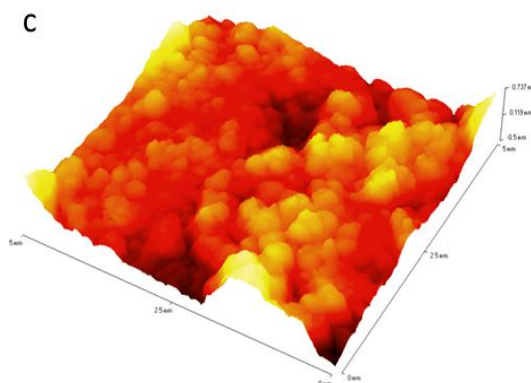


**Figure 4.9** AFM images of unmodified electrode (a), G/PANI nanocomposite modified electrode (b), and electropolymerized aniline on G/PANI nanocomposite modified electrode (c).

#### 4.2.2 Electrochemical characterization

The electrochemical characteristics of the modified electrode were monitored by cyclic voltammetry, using a standard  $[\text{Fe}(\text{CN})_6]^{3-/4-}$  redox couple. As shown in Figure 4.10, cyclic voltammetry was performed on different electrodes consisting of electropolymerized aniline on G/PANI nanocomposite modified electrode, G/PANI nanocomposite modified electrode, and unmodified electrode. The anodic and cathodic peak currents of  $[\text{Fe}(\text{CN})_6]^{3-/4-}$  showed the well-defined peaks for all electrodes. The highest anodic and cathodic peak current was performed on the electropolymerized aniline on G/PANI modified electrode (red line) which was approximately 4 times higher than the unmodified electrode (green line) and 2 times higher than the G/PANI nanocomposite modified electrode (blue line). These results exhibit that the electropolymerized aniline on G/PANI modified electrode improves the electrochemical sensitivity of the system. The peak potential difference values ( $\Delta E_p$ ) of standard  $[\text{Fe}(\text{CN})_6]^{3-/4-}$  measured on electropolymerized aniline on G/PANI modified electrode ( $\Delta E_p=0.45$ ; red line) decreased when compared with  $\Delta E_p$  from an unmodified electrode ( $\Delta E_p=0.66$ ; green line). The modified electrode can expedite the electron transfer process of system. Then, the electropolymerized aniline on G/PANI nanocomposite modified electrode was

applied for capture antibody immobilization and NGAL determination by using cyclic voltammetry.

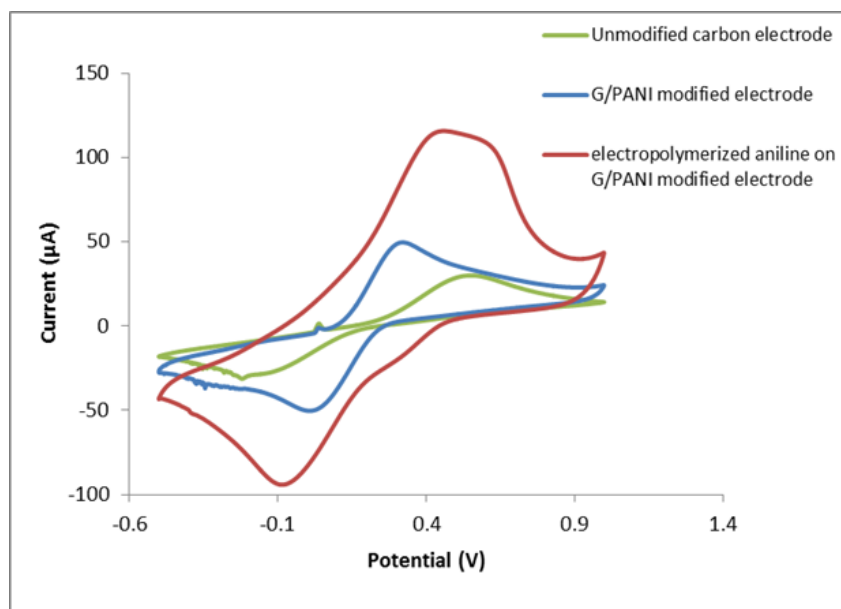


**Figure 4.10** Cyclic voltammograms of 1.0 mM  $[\text{Fe}(\text{CN})_6]^{3-/4-}$  at 100 mV/s with the unmodified screen-printed carbon electrode (green line), G/PANI nanocomposite modified carbon electrode (blue line) and electropolymerized aniline on G/PANI nanocomposite modified electrode (red line).

#### 4.3 The performance of the electropolymerized aniline on G/PANI nanocomposite modified electrodes

The electrochemical behaviors of G/PANI/PS nanoporous fiber modified carbon electrodes were studied by using  $[\text{Fe}(\text{CN})_6]^{3-/4-}$  as a standard redox couple. The cyclic voltammetric measurements were performed at different scan rates. For diffusion controlled mass-transfer electrode process, the peak current and square root of scan rate ( $v^{1/2}$ ) is linear (Randles-Sevcik equation). As scan rate increased, the anodic and cathodic peak currents increase. The linear relationship between peak current and  $v^{1/2}$  plotted in the range from 50-100 mV/s (Figure 4.11).

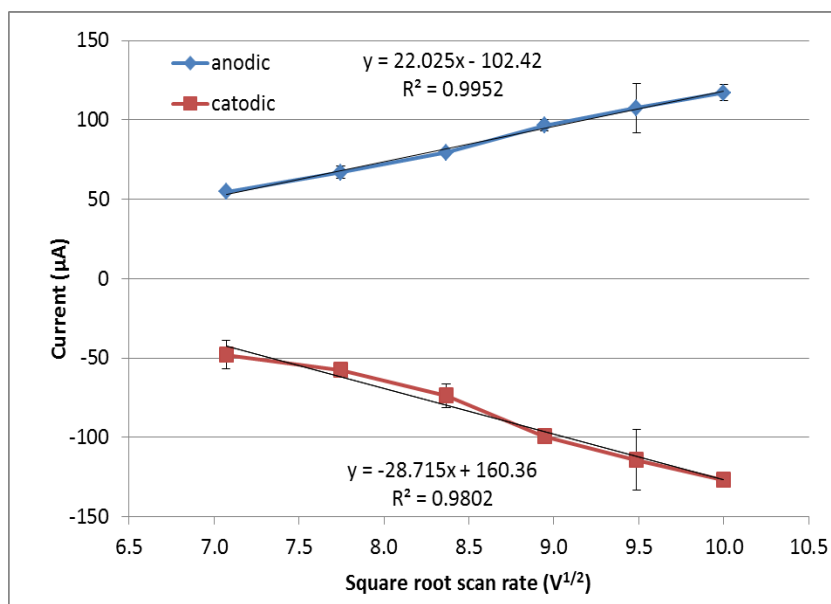


**Figure 4.11** The relationship between the square root of scan rate ( $V^{1/2}$ ) and peak currents.

#### 4.4 NGAL Detection

##### 4.4.1 Cyclic voltammetry

Cyclic voltammetry was used to detect NGAL. Firstly NGAL antibody was immobilized on the modified electrode via covalent bonding using EDC/NHS coupling agent for specific detection of NGAL protein. The cyclic voltammograms of NGAL and background measured on electropolymerization of aniline on G/PANI nanocomposite modified electrode were shown in Figure 4.12. Along with cyclic voltammogram of NGAL, the NGAL antibody incorporated with electropolymerized aniline on G/PANI nanocomposite modified electrode shows a broad oxidation peak for NGAL around 0-0.6 V. A dramatic increase in the anodic current signal of 90 ng/ml of NGAL in 0.1 M phosphate buffer solution pH 7.0 at scan rate 0.5 V is observed (blue line) when compared to the background current signal (0.1 M phosphate buffer solution; red line), indicating that the electropolymerization of aniline on G/PANI nanocomposite modified electrode might be electrocatalyst for sensitive detection of NGAL.

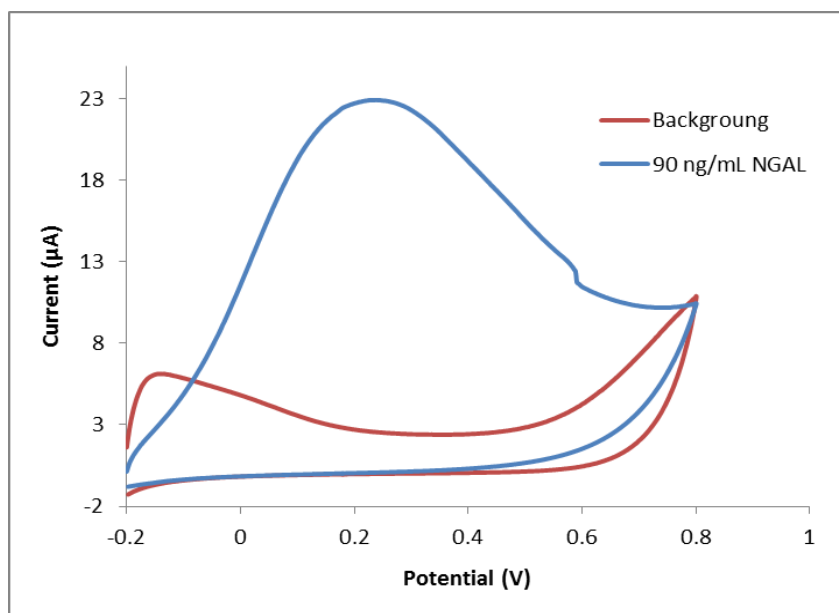


**Figure 4.12** Cyclic voltammogram of electropolymerized aniline on G/PANI nanocomposite modified electrode in the absent (Blue) and present (Red) of 90 ng/mL of NGAL in phosphate buffer solution (pH 7.0) at scan rate 50 mV/s.

The performances of modified electrode for NGAL detection were studied. Three different electrodes including unmodified carbon electrode, G/PANI nanocomposite modified electrode and electropolymerized aniline on G/PANI nanocomposite modified electrode were shown in Figure 4.13. The oxidation peak current of NGAL on electropolymerized aniline on G/PANI nanocomposite modified electrode is higher than unmodified electrode and G/PANI nanocomposite modified electrode because the amount of aniline on the electrode surface improves the specific binding of antibody on the electrode surface and thus increases the performance for NGAL detection.

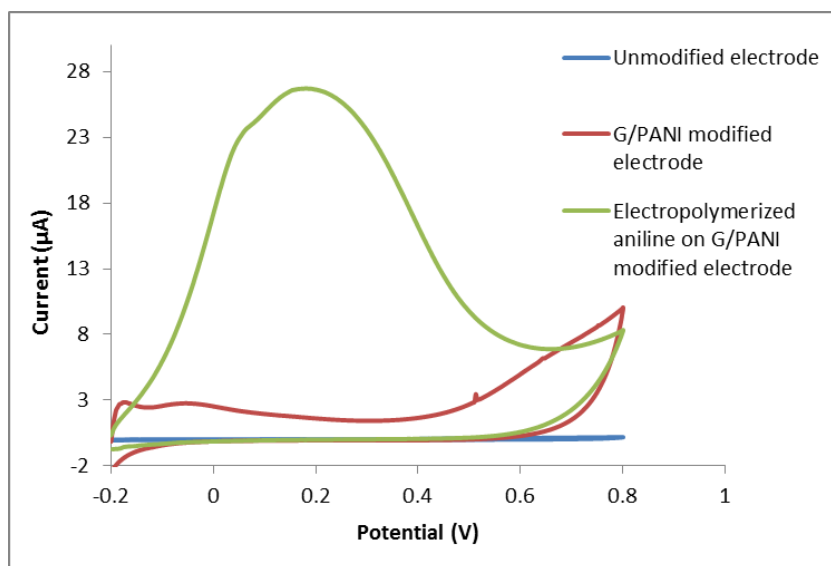


**Figure 4.13** Cyclic voltammogram of 200 ng/mL NGAL with unmodified electrode (blue), G/PANI nanocomposite modified electrode (red), electropolymerized aniline on G/PANI nanocomposite modified electrode (green).

#### 4.4.2 Amperometry

After characterization of electropolymerized aniline on G/PANI nanocomposite modified electrode using cyclic voltammetry, the determination of NGAL was conducted using chronoamperometry. Chronoamperometry was selected for the determination of NGAL due to its high sensitivity and wide applicability. In this study, hydrodynamic voltammetry was optimized by adjusting the detection potential in a range of 0.1-0.6 V as shown in Figure 4.14. The anodic current signal of NGAL significantly decreases when the detection potential increases from 0 to +0.3 V, after that the anodic current signal slightly increases when the detection potential increases from 0.3 to 0.6 V; however, the background current also increases. Consequently, a signal-to-background ratio (S/B) from hydrodynamic voltammogram was considered. Figure 4.15 showed the S/B ratio at different detection potentials. 0.3 V as a detection potential was selected for further studies because it shows the highest S/B ratio for NGAL detection.

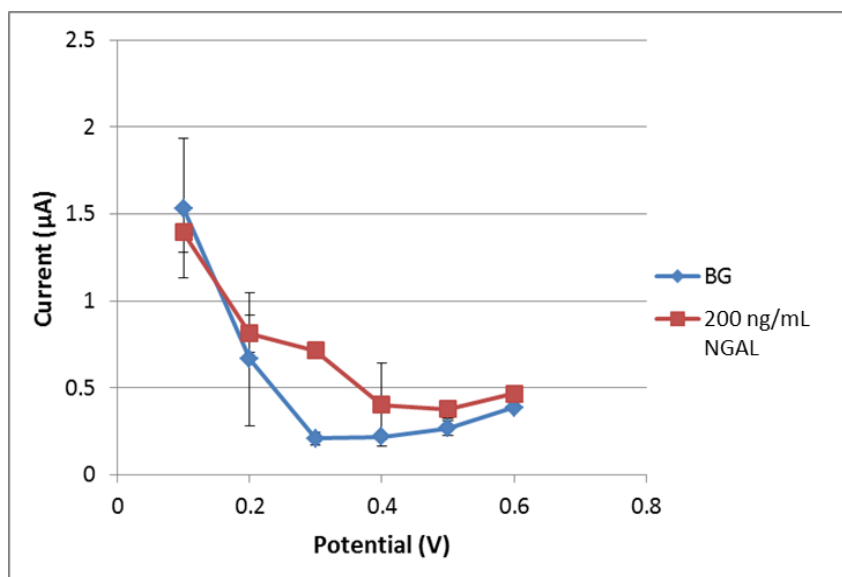


**Figure 4.14** A hydrodynamic voltammograms of 200 ng/mL of NGAL (red line) and background (blue line) in 0.1 M PBS pH 7.0 at a 75 s measured on electropolymerized aniline on G/PANI nanacomposite modified electrode.

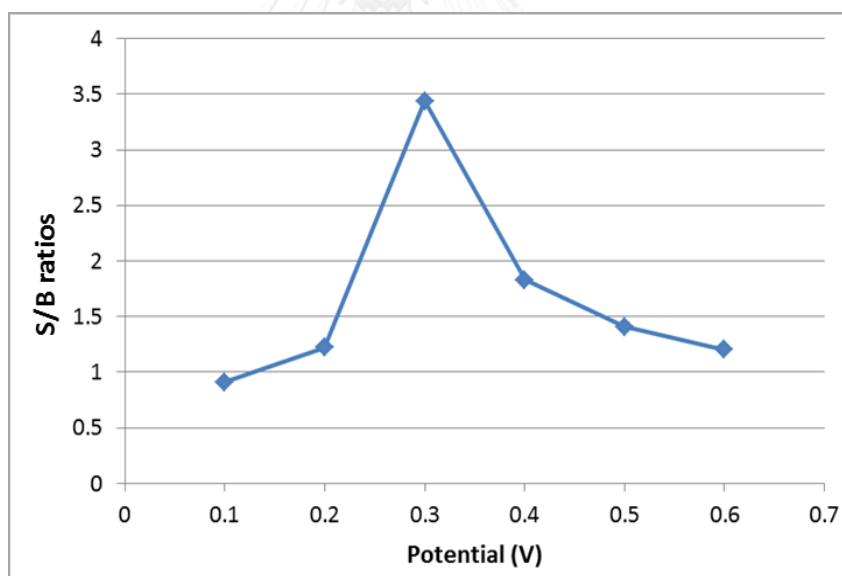


**Figure 4.15** Hydrodynamic voltammogram of the signal-to-background ratios (S/B) at different detection potential (0.1-0.6 V).

#### 4.5 Calibration curve

The electrochemical responses of electropolymerized aniline on G/PANI nanacomposite modified electrode were measured at different concentrations of NGAL protein (50-500 ng/ml). For amperometric detection, the current responses were recorded at 75 s as a steady state to create a calibration curve for NGAL determination. As shown in Figure 4.16, the calibration curve was obtained as a functional of NGAL concentration. A linearly relationship between current response and NGAL concentration was performed in the range of 50 to 500 ng/mL with a correlation coefficient ( $R^2$ ) of 0.9984. Limit of detection (LOD) was calculated by using  $LOD=3S_b/m$  equation, limit of detection (LOD) was calculated using the equation of  $LOD=10S_b/m$ , when  $S_b$  is a standard deviation of the blank (estimated by five replicates determination of the blank signals) and  $m$  is a slope of calibration curve. The limit of detection (LOD) and the limit of quantitation (LOQ) for NGAL determination were 21.13 ng/mL and 70.44 ng/mL, respectively. Eventually, this proposed system was applied for the detection of NGAL in human urine sample.

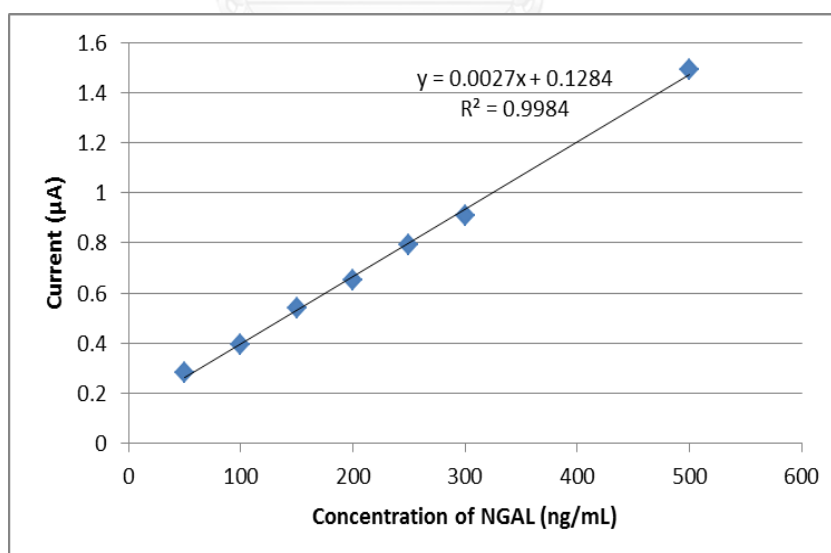


**Figure 4.16** The calibration curve for detection of NGAL in the concentration range of 50 – 500 ng/mL in 0.1 M PBS (pH 7.0)



#### 4.6 Interference study

In human urine, many substances, such as bovine serum albumin (BSA) can potentially interfere the detection of NGAL. Thus, the selectivity of this proposed system was studied. For the assessment of BSA interference, various concentration of BSA was incubated on the electropolymerized aniline on G/PANI nanocomposite modified electrode. After washing the excess BSA using PBS and milliQ water, the current signal of NGAL in the presence of BSA was recorded and compared with background and 100 ng/ml of NGAL (in the absence of BSA). The oxidation current of NGAL in the presence of BSA shows a negligible effect on the current response as showed in Figure 4.17.

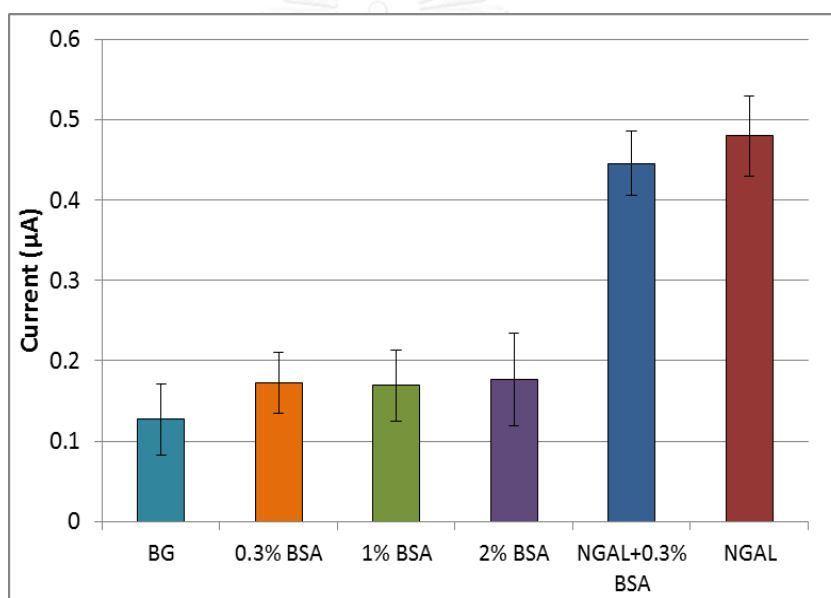


**Figure 4.17** The interference effect of BSA in PB solution and 100 ng/mL of NGAL.

#### 4.7 Real sample

To evaluate the performance of this proposed system, electropolymerized aniline on G/PANI nanocomposite modified electrode was used for the determination of NGAL in human urine samples. The human urine samples were centrifuge at 1600 rpm for 20 min, and the supernatants were kept for amperometric analysis using the modified electrode. The standard solutions of the NGAL were added into sample in the ratio of 1:1 and used for further detection. The percentages of recoveries (Table

4.1) were found in a range of 97.45–104.37 % and the RSD was less than 5.0%. The accuracy of this system was investigated by compared with the ELISA method as a validation method (Table 4.2). The modified electrode was applied to measure NGAL in patient urine samples. The % recoveries were found in the range of 93.51-104.30 %, verifying that this sensing system is highly accurate.

**Table 4.1** Determination of NGAL in human urine sample.

Added (ng/mL)	Found (ng/mL)	Recovery (%)
100	97.45 ± 0.98	97.45
200	208.73 ± 1.41	104.37
400	413.4 ± 2.12	103.25

**Table 4.2** Determination of NGAL in patient urine sample.

Urine samples	ELISA (ng/mL)	Found (ng/mL)	Recovery (%)
1	200.00	199.50 ± 13.47	99.75
2	1645.00	1642.00 ± 14.67	93.51

#### 4.8 Reproducibility and stability

The reproducibility and stability of the electropolymerized aniline on G/PANI nanocomposite modified electrode were investigated by using amperometric detection of 200 ng/mL of NGAL. The relative standard deviations (RSD) of NGAL concentrations were found between 1.49-9.20%. The RSD showed acceptable reproducibility for this system. For stability of the system the electropolymerized aniline on G/PANI nanocomposite modified electrode were kept in PBS (pH 7.0) at a room temperature. The current respond decreased 2-9% in 1-3 day at a room temperature. In this study, the results showed that the electropolymerized aniline on G/PANI nanocomposite modified electrode is relatively stable for NGAL detection.

## CHAPTER V

### CONCLUSION

#### 5.1 Conclusion

In this study, electropolymerized aniline on G/PANI nanodroplet modified electrodes were successfully prepared and used for the sensitive determination of NGAL protein. For electrospray fabrication of G/PANI nanodroplet modified electrode, a high voltage of 7.5 kV was applied to the solution with a flow rate of 1.0 mL/h and 5 cm distance between needle and ground collector.

The optimal parameters for electropolymerized aniline on G/PANI nanodroplet modified electrode include scan number of 4 cycles and 0.10 M of aniline concentration at a scan rate of 100 mV/s.

Under the optimum conditions, a high-sensitivity, wide linear range and low limit of detection for NGAL detection was achieved. The calibration plot is linearly proportional to NGAL concentration in a range of 50-250 ng/mL. Limit of detection (LOD) and limit of quantitation (LOQ) for NGAL were found to be 21 ng/mL and 50 ng/mL, respectively. Moreover, the results obtained from our system correspond well with the results obtained from ELISA. Eventually, this proposed system was successfully applied for the determination of NGAL in human urine and the percent recoveries were found to be 97.45–104.37%.

#### 5.2 Suggestion for future work

This novel immunosensor based on electropolymerized aniline on G/PANI nanodroplet modified electrode might be an alternative tool for early stage diagnosis of acute kidney injury.

The better understanding of antigen-antibody binding mechanism on electrochemical signal (e.g. molecular modeling) and further system optimization, such as increasing amount of amino group along with improving electrochemical sensitivity might make this sensing platform very useful for other types of biosensors and thus biomedical devices.

## REFERENCES

- [1] Mandelbaum, T., Scott, D.J., Lee, J., Mark, R.G., Malhotra, A., Waikar, S.S., Howell, M.D., and Talmor, D. Outcome of critically ill patients with acute kidney injury using the Acute Kidney Injury Network criteria. Crit Care Med 39(12) (2011): 2659-64.
- [2] Himmelfarb, J. and Ikizler, T.A. Acute kidney injury: changing lexicography, definitions, and epidemiology. Kidney Int 71(10) (2007): 971-976.
- [3] Shusterman, N., Strom, B.L., Murray, T.G., Morrison, G., West, S.L., and Maislin, G. Risk factors and outcome of hospital-acquired acute renal failure: Clinical Epidemiologic Study. The American Journal of Medicine 83(1) (1987): 65-71.
- [4] Cruz, D.N., Bolgan, I., Perazella, M.A., Bonello, M., de Cal, M., Corradi, V., Polanco, N., Ocampo, C., Nalesso, F., Piccinni, P., and Ronco, C. North East Italian Prospective Hospital Renal Outcome Survey on Acute Kidney Injury (NEiPHROS-AKI): targeting the problem with the RIFLE Criteria. Clin J Am Soc Nephrol 2(3) (2007): 418-25.
- [5] Becherucci, F., Mazzinghi, B., Ronconi, E., Peired, A., Lazzeri, E., Sagrinati, C., Romagnani, P., and Lasagni, L. The role of endothelial progenitor cells in acute kidney injury. Blood purification 27(3) (2009): 261-70.
- [6] Zappitelli, M., Bernier, P.-L., Saczkowski, R.S., Tchervenkov, C.I., Gottesman, R., Dancea, A., Hyder, A., and Alkandari, O. A small post-operative rise in serum creatinine predicts acute kidney injury in children undergoing cardiac surgery. Kidney Int 76(8) (2009): 885-892.
- [7] Weisbord, S.D., Chen, H., Stone, R.A., Kip, K.E., Fine, M.J., Saul, M.I., and Palevsky, P.M. Associations of increases in serum creatinine with mortality and length of hospital stay after coronary angiography. J Am Soc Nephrol 17(10) (2006): 2871-7.
- [8] Bagshaw, S.M., Uchino, S., Cruz, D., Bellomo, R., Morimatsu, H., Morgera, S., Schetz, M., Tan, I., Bouman, C., Macedo, E., Gibney, N., Tolwani, A., Oudemans-van Straaten, H.M., Ronco, C., and Kellum, J.A. A comparison of

- observed versus estimated baseline creatinine for determination of RIFLE class in patients with acute kidney injury. Nephrol Dial Transplant 24(9) (2009): 2739-44.
- [9] Zappitelli, M., Bernier, P.L., Saczkowski, R.S., Tchervenkov, C.I., Gottesman, R., Dancea, A., Hyder, A., and Alkandari, O. A small post-operative rise in serum creatinine predicts acute kidney injury in children undergoing cardiac surgery. Kidney Int 76(8) (2009): 885-92.
- [10] Wagener, G., Jan, M., Kim, M., Mori, K., Barasch, J.M., Sladen, R.N., and Lee, H.T. Association between increases in urinary neutrophil gelatinase-associated lipocalin and acute renal dysfunction after adult cardiac surgery. Anesthesiology 105(3) (2006): 485-91.
- [11] Royackers, A.A., Korevaar, J.C., van Suijlen, J.D., Hofstra, L.S., Kuiper, M.A., Spronk, P.E., Schultz, M.J., and Bouman, C.S. Serum and urine cystatin C are poor biomarkers for acute kidney injury and renal replacement therapy. Intensive Care Med 37(3) (2011): 493-501.
- [12] Hobson, C.E., Yavas, S., Segal, M.S., Schold, J.D., Tribble, C.G., Layon, A.J., and Bihorac, A. Acute kidney injury is associated with increased long-term mortality after cardiothoracic surgery. Circulation 119(18) (2009): 2444-53.
- [13] Devarajan, P. Emerging biomarkers of acute kidney injury. Contrib Nephrol 156 (2007): 203-12. CHULALONGKORN UNIVERSITY
- [14] Hall, I.E., Yarlagadda, S.G., Coca, S.G., Wang, Z., Doshi, M., Devarajan, P., Han, W.K., Marcus, R.J., and Parikh, C.R. IL-18 and urinary NGAL predict dialysis and graft recovery after kidney transplantation. J Am Soc Nephrol 21(1) (2010): 189-97.
- [15] Nguyen, M. and Devarajan, P. Biomarkers for the early detection of acute kidney injury. Pediatric Nephrology 23(12) (2008): 2151-2157.
- [16] Devarajan, P. Review: neutrophil gelatinase-associated lipocalin: a troponin-like biomarker for human acute kidney injury. Nephrology (Carlton) 15(4) (2010): 419-28.
- [17] Devarajan, P. Neutrophil gelatinase-associated lipocalin: a promising biomarker for human acute kidney injury. Biomarkers in medicine 4(2) (2010): 265-280.

- [18] Mishra, J., Dent, C., Tarabishi, R., Mitsnefes, M.M., Ma, Q., Kelly, C., Ruff, S.M., Zahedi, K., Shao, M., Bean, J., Mori, K., Barasch, J., and Devarajan, P. Neutrophil gelatinase-associated lipocalin (NGAL) as a biomarker for acute renal injury after cardiac surgery. The Lancet 365(9466): 1231-1238.
- [19] Cemil, K., Elif, C., Serkan, Y.M., Fevzi, Y., Deniz, A.E., Tamer, D., and Polat, D. The value of serum NGAL in determination of dialysis indication. J Pak Med Assoc 64(7) (2014): 739-42.
- [20] Segev, G., Palm, C., LeRoy, B., Cowgill, L.D., and Westropp, J.L. Evaluation of neutrophil gelatinase-associated lipocalin as a marker of kidney injury in dogs. J Vet Intern Med 27(6) (2013): 1362-7.
- [21] Kjeldsen, L., Johnsen, A.H., Sengelov, H., and Borregaard, N. Isolation and primary structure of NGAL, a novel protein associated with human neutrophil gelatinase. J Biol Chem 268(14) (1993): 10425-32.
- [22] Dent, C.L., Ma, Q., Dastrala, S., Bennett, M., Mitsnefes, M.M., Barasch, J., and Devarajan, P. Plasma neutrophil gelatinase-associated lipocalin predicts acute kidney injury, morbidity and mortality after pediatric cardiac surgery: a prospective uncontrolled cohort study. Critical Care 11(6) (2007): R127-R127.
- [23] Hirsch, R., Dent, C., Pfriem, H., Allen, J., Beekman, R.H., 3rd, Ma, Q., Dastrala, S., Bennett, M., Mitsnefes, M., and Devarajan, P. NGAL is an early predictive biomarker of contrast-induced nephropathy in children. Pediatric Nephrology 22(12) (2007): 2089-95.
- [24] Grieshaber, D., MacKenzie, R., Vörös, J., and Reimhult, E. Electrochemical Biosensors - Sensor Principles and Architectures. Sensors (Basel, Switzerland) 8(3) (2008): 1400-1458.
- [25] Thévenot, D.R., Toth, K., Durst, R.A., and Wilson, G.S. Electrochemical biosensors: recommended definitions and classification1. Biosensors and Bioelectronics 16(1-2) (2001): 121-131.
- [26] Promphet, N., Rattanarat, P., Rangkupan, R., Chailapakul, O., and Rodthongkum, N. An electrochemical sensor based on graphene/polyaniline/polystyrene nanoporous fibers modified electrode for

- simultaneous determination of lead and cadmium. Sensors and Actuators B: Chemical 207, Part A(0) (2015): 526-534.
- [27] Ruecha, N., Rangkupan, R., Rodthongkum, N., and Chailapakul, O. Novel paper-based cholesterol biosensor using graphene/polyvinylpyrrolidone/polyaniline nanocomposite. Biosensors and Bioelectronics 52(0) (2014): 13-19.
- [28] Thammasoontaree, N., Rattanarat, P., Ruecha, N., Siangproh, W., Rodthongkum, N., and Chailapakul, O. Ultra-performance liquid chromatography coupled with graphene/polyaniline nanocomposite modified electrode for the determination of sulfonamide residues. Talanta 123(0) (2014): 115-121.
- [29] Rodthongkum, N., Ruecha, N., Rangkupan, R., Vachet, R.W., and Chailapakul, O. Graphene-loaded nanofiber-modified electrodes for the ultrasensitive determination of dopamine. Analytica Chimica Acta 804(0) (2013): 84-91.
- [30] Zhang, B.-T., Zheng, X., Li, H.-F., and Lin, J.-M. Application of carbon-based nanomaterials in sample preparation: A review. Analytica Chimica Acta 784(0) (2013): 1-17.
- [31] Rao, K.S., Senthilnathan, J., Liu, Y.-F., and Yoshimura, M. Role of Peroxide Ions in Formation of Graphene Nanosheets by Electrochemical Exfoliation of Graphite. Sci. Rep. 4 (2014).
- [32] Bo, Y., Yang, H., Hu, Y., Yao, T., and Huang, S. A novel electrochemical DNA biosensor based on graphene and polyaniline nanowires. Electrochimica Acta 56(6) (2011): 2676-2681.
- [33] Fan, Y., Liu, J.-H., Yang, C.-P., Yu, M., and Liu, P. Graphene–polyaniline composite film modified electrode for voltammetric determination of 4-aminophenol. Sensors and Actuators B: Chemical 157(2) (2011): 669-674.
- [34] Grieshaber, D., MacKenzie, R., Vörös, J., and Reimhult, E. Electrochemical Biosensors - Sensor Principles and Architectures. Sensors 8(3) (2008): 1400-1458.
- [35] Ferreira, A.A.P., Uliana, C.V., Castilho, M.d.S., Pesquero, N.C., Foguel, M.V., Santos, G.P.d., Fugivara, C.S., Benedetti, A.V., and Yamanaka, H. Amperometric

- Biosensor for Diagnosis of Disease. State of the Art in Biosensors - Environmental and Medical Applications. 2013.
- [36] Ybarra, C.M.G. Fundamentals and Applications of Immunosensors, Advances in Immunoassay Technology. InTech, 2012
- [37] Kissinger, P.T. and Heineman, W.R. Cyclic voltammetry. Journal of Chemical Education 60(9) (1983): 702.
- [38] Andrade, A.S.O., Maria D.L., Faulin, T.E.S., Hering, V.R., and Abdalla, D.S.P. Biosensors for Health, Environment and Biosecurity, ed. Serra, P.A.: InTech, 2011.
- [39] Gau, V., Ma, S.-C., Wang, H., Tsukuda, J., Kibler, J., and Haake, D.A. Electrochemical molecular analysis without nucleic acid amplification. Methods 37(1) (2005): 73-83.
- [40] Bard, A.J. and Faulkner, L.R. Fundamentals and Applications. 2nd ed. New York, USA: John Wiley & Sons, 2001.
- [41] Radhapyari, K., Kotoky, P., Das, M.R., and Khan, R. Graphene–polyaniline nanocomposite based biosensor for detection of antimalarial drug artesunate in pharmaceutical formulation and biological fluids. Talanta 111(0) (2013): 47-53.
- [42] Xing, X., Liu, S., Yu, J., Lian, W., and Huang, J. Electrochemical sensor based on molecularly imprinted film at polypyrrole-sulfonated graphene/hyaluronic acid-multiwalled carbon nanotubes modified electrode for determination of tryptamine. Biosensors and Bioelectronics 31(1) (2012): 277-283.
- [43] Bora, C. and Dolui, S.K. Fabrication of polypyrrole/graphene oxide nanocomposites by liquid/liquid interfacial polymerization and evaluation of their optical, electrical and electrochemical properties. Polymer 53(4) (2012): 923-932.
- [44] Wisitsoraat, A., Pakapongpan, S., Sriprachuabwong, C., Phokharatkul, D., Sritongkham, P., Lomas, T., and Tuantranont, A. Graphene–PEDOT:PSS on



- screen printed carbon electrode for enzymatic biosensing. Journal of Electroanalytical Chemistry 704(0) (2013): 208-213.
- [45] Wang, G.-X., Qian, Y., Cao, X.-X., and Xia, X.-H. Direct electrochemistry of cytochrome c on a graphene/poly (3,4-ethylenedioxythiophene) nanocomposite modified electrode. Electrochemistry Communications 20(0) (2012): 1-3.
- [46] Dhand, C., Das, M., Datta, M., and Malhotra, B.D. Recent advances in polyaniline based biosensors. Biosensors and Bioelectronics 26(6) (2011): 2811-2821.
- [47] Ćirić-Marjanović, G. Recent advances in polyaniline research: Polymerization mechanisms, structural aspects, properties and applications. Synthetic Metals 177(0) (2013): 1-47.
- [48] Zhenjing Zhuang, Jianyong Li, Ruian Xu, and Dan Xiao. Electrochemical Detection of Dopamine in the Presence of Ascorbic Acid Using Overoxidized Polypyrrole/Graphene Modified Electrodes. Int. J. Electrochem. Sci. 6 (2011): 2149 - 2161.
- [49] Xu, Q., Gu, S.-X., Jin, L., Zhou, Y.-e., Yang, Z., Wang, W., and Hu, X. Graphene/polyaniline/gold nanoparticles nanocomposite for the direct electron transfer of glucose oxidase and glucose biosensing. Sensors and Actuators B: Chemical 190(0) (2014): 562-569.
- [50] Nathalie Bock, M.A.W., Dietmar W. Huttmacher, and Tim R. Dargaville. Electrospraying, a Reproducible Method for Production of Polymeric Microspheres for Biomedical Applications. Polymers 3 (2011): 131-149.
- [51] Amit Jadhav and Lijing Wang, R.P. Influence of Applied Voltage on Droplet Size Distribution in Electrospraying of Thermoplastic Polyurethan. International Journal of Materials, Mechanics and Manufacturing 1 (2013): 287-289.
- [52] Coca, S.G., Yusuf, B., Shlipak, M.G., Garg, A.X., and Parikh, C.R. Long-term Risk of Mortality and Other Adverse Outcomes After Acute Kidney Injury: A

- Systematic Review and Meta-analysis. American Journal of Kidney Diseases 53(6) (2009): 961-973.
- [53] Fang, Y., Ding, X., Zhong, Y., Zou, J., Teng, J., Tang, Y., Lin, J., and Lin, P. Acute kidney injury in a Chinese hospitalized population. Blood purification 30(2) (2010): 120-126.
- [54] Waikar, S.S., Liu, K.D., and Chertow, G.M. Diagnosis, epidemiology and outcomes of acute kidney injury. Clin J Am Soc Nephrol 3(3) (2008): 844-61.
- [55] Ishani, A., Xue, J.L., Himmelfarb, J., Eggers, P.W., Kimmel, P.L., Molitoris, B.A., and Collins, A.J. Acute kidney injury increases risk of ESRD among elderly. J Am Soc Nephrol 20(1) (2009): 223-8.
- [56] Rosner, M. Acute Kidney Injury Associated with Cardiac Surgery. in Machiraju, V.R., Schaff, H.V., and Svensson, L.G. (eds.), Redo Cardiac Surgery in Adults, pp. 37-52: Springer New York, 2012.
- [57] Gabbard, W., Milbrandt, E.B., and Kellum, J.A. NGAL: an emerging tool for predicting severity of AKI is easily detected by a clinical assay. Critical Care 14(4) (2010): 318-318.
- [58] Vashist, S.K. Graphene-based immunoassay for human lipocalin-2. Analytical Biochemistry 446(0) (2014): 96-101.
- [59] Kannan, P., Tiong, H.Y., and Kim, D.-H. Highly sensitive electrochemical determination of neutrophil gelatinase-associated lipocalin for acute kidney injury. Biosensors and Bioelectronics 31(1) (2012): 32-36.
- [60] Csernok, E. and Moosig, F. Current and emerging techniques for ANCA detection in vasculitis. Nat Rev Rheumatol 10(8) (2014): 494-501.

## VITA

Jutiporn Yukird was born in December 28, 1989 in Surin, Thailand. She received her Bachelor Degree of Science Program in chemistry from Srinakharinwirot University, Bangkok, Thailand (2008-2012) and expect graduated her Master Degree of Science program in Petrochemical and Polymer Science from Chulalongkorn University, Bangkok, Thailand in 2014.

### Poster presentations

1. Yukird, J., Rangkupan, R., Pisitkun, T. Rodthongkum, N., Chailapakul, O. "Graphene/polyaniline nanocomposite modified electrode for biosensors" International Bioscience Conference 2014 (IBSC 2014) September 29-30, 2014, Phuket, Thailand

2. Yukird, J., Rangkupan, R., Pisitkun, T. Rodthongkum, N., Chailapakul, O. "A Novel Electrochemical Biosensor Based on Graphene/Polyaniline Nanocomposite Modified Electrode" The 3rd International Symposium on Fundamental and Applied Sciences (ISFAS) March 22-24, 2015, Osaka, Japan

3. Chailapakul, O., Yukird, J., Rodthongkum, N., Rangkupan, R., Pisitkun, T. "Graphene/polyaniline nanocomposite modified electrode for biosensors" Techconnect World Innovation Conference 2014 & Expo (Techconnect 2014) June 15-18, 2014, Washington, DC

### Proceedings

1. Chailapakul, O., Yukird, J., Rodthongkum, N., Rangkupan, R., Pisitkun, T. Graphene/polyaniline nanocomposite modified electrode for biosensors, Nanotech 2014 (1):76 - 79.

2. Yukird, J., Rangkupan, R., Pisitkun, T. Rodthongkum, N., Chailapakul, O. Graphene/polyaniline nanocomposite modified electrode for biosensors, Proceedings of International Bioscience Conference 2014. 2014:375-378